HHS Public Access

Author manuscript

Nature. Author manuscript; available in PMC 2015 June 19.

Published in final edited form as:

Nature. 2014 August 21; 512(7514): 328–332. doi:10.1038/nature13428.

Dynamic pathways of -1 translational frameshifting

Jin Chen[1,2], **Alexey Petrov**[2], **Magnus Johansson**[2], **Albert Tsai**[1,2], **Seán E. O'Leary**[2], and **Joseph D. Puglisi**[2]

[1]Department of Applied Physics, Stanford University, Stanford, CA, USA

[2]Department of Structural Biology, Stanford University School of Medicine, Stanford, CA, USA

Abstract

Spontaneous changes in the reading frame of translation are rare (frequency of 10^{-3} – 10^{-4} per codon)[1], but can be induced by specific features in the messenger RNA (mRNA). In the presence of mRNA secondary structures, a heptanucleotide "slippery sequence" usually defined by the motif X XXY YYZ, and (in some prokaryotic cases) mRNA sequences that base pair with the 3′ end of the 16S ribosomal rRNA (internal Shine-Dalgarno (SD) sequences), there is an increased probability that a specific programmed change of frame occurs, wherein the ribosome shifts one nucleotide backwards into an overlapping reading frame (−1 frame) and continues by translating a new sequence of amino acids[2,3]. Despite extensive biochemical and genetic studies, there is no clear mechanistic description for frameshifting. Here, we apply single-molecule fluorescence to track the compositional and conformational dynamics of the individual ribosomes at each codon during translation of a frameshift-inducing mRNA from the *dnaX* gene in *Escherichia coli*. Ribosomes that frameshift into the −1 frame are characterized by a 10-fold longer pause in elongation compared to non-frameshifted ribosomes, which translate through unperturbed. During the pause, interactions of the ribosome with the mRNA stimulatory elements uncouple EF-G catalyzed translocation from normal ribosomal subunit reverse-rotation, leaving the ribosome in a non-canonical intersubunit rotated state with an exposed codon in the aminoacyl-tRNA site (A site). $tRNA^{Lys}$ sampling and accommodation to the empty A site either lead to the slippage of the tRNAs into the −1 frame or maintain the ribosome into the 0 frame. Our results provide a general mechanistic and conformational framework for −1 frameshifting, highlighting multiple kinetic branchpoints during elongation.

Despite detailed biochemical and genetic studies, the mechanism of −1 programmed ribosomal frameshifting (PRF) remains poorly understood with various models to explain frameshifting[2,4–11]. The 3′-hairpin[12] and 5′-internal-SD sequence[13] (in some prokaryotic cases) pause the ribosome over the slippery sequence, which is necessary but not sufficient

Correspondence should be addressed to J.D.P., puglisi@stanford.edu Phone: 650-498-4397.

AUTHOR CONTRIBUTIONS

J.C. performed all the experiments and the data analysis. J.C., A.P., and J.D.P. designed the project and wrote the manuscript. M.J. and S.E.O'L. assisted with reagent preparation. All authors discussed the results and commented on the manuscript.

COMPETING FINANCIAL INTERESTS

The authors declare no competing financial interests.

to drive efficient −1 PRF. How these structural elements induce the pause and operate together to manipulate the ribosomal reading frame are not known. During a −1 frameshift, the anticodons of the tRNAs must detach from the mRNA and re-associate in the −1 frame. However, this slippage may occur at distinct points during the elongation cycle: (1) during accommodation of the A-site tRNA[4], (2) subsequent to accommodation, but prior to peptidyl transfer[8], (3) during EF-G catalyzed translocation[9,10], or (4) after translocation but before the next round of elongation[11]. Since the exact timing of frameshifting is unknown, the precise position of the ribosome over slippery sequence during the slippage is unclear[8,11]. Finally, since −1 PRF occurs at usually 1~80% efficiency depending on the sequence[10], what determines whether one particular ribosome will frameshift or not remains elusive.

The dynamic and stochastic nature of frameshifting requires direct observation of single ribosomes translating multiple codons of an mRNA. We harness here single-molecule fluorescence and zero-mode waveguides (ZMWs) instrumentation[14] to track ribosome progression on mRNAs and observe −1 translational frameshifting in real-time[15]. Conformational changes underlying elongation, involving rotational movements of the small (30S) ribosomal subunit body with respect to the large (50S) ribosomal subunit, were monitored during translation by site-specifically labeling the 30S with Cy3B and 50S with BHQ-2 (a nonfluorescent quencher), allowing for Förster resonance energy transfer (FRET) between the two dyes[16,17]. During normal translation elongation, aminoacyl-tRNA-EF-Tu-GTP ternary complex (TC) accommodation to the A site followed by peptide bond formation drives the nonrotated to rotated state transition (low to high Cy3B intensity, or high to low FRET) whereas EF-G catalyzed translocation drives the rotated to nonrotated transition (high to low Cy3B intensity)[16]. Thus, one round of high-low-high FRET (low-high-low Cy3B intensity) corresponds to a single ribosome translating one codon (see Extended Data Fig. 1)[16,18]. Arrival and departure of the dye-labeled ligands such as Cy5-tRNAs and EF-G can be simultaneously observed as a sequence of fluorescent pulses[16,17]. We applied this approach to the −1 frameshift sequence from the *dnaX* gene in the *E. coli*, which contains an internal SD sequence, and a slippery -A AAA AAG- sequence followed by a RNA hairpin[3,12,13].

We observed −1 frameshifting directly on a *dnaX* frameshift sequence, designed such that ribosomes that frameshift will translate 9 codons and stop at a stop codon in the −1 frame, while ribosomes that do not frameshift will translate 12 codons until a stop codon in the 0 frame (Fig. 1a). By delivering total tRNA ($tRNA_{tot}$) ternary complex, EF-G, and BHQ-50S to immobilized Cy3B-30S preinitiation complexes (30S subunit-mRNA-initiator tRNA), we observe ribosomes that translate either the full 12 codons or only 9 codons, as measured by the number of intersubunit FRET cycles (see Extended Data Fig. 2). By determining the fraction of ribosomes that translate > 9 codons, or translate up to 9 codons, we obtain an estimate of the frameshifting percentage (~75%), consistent with previously observed frameshifting efficiency[13] (confirmed independently as shown in Extended Data Fig. 2b, c). The SD sequence and hairpin act as barriers to translocation, so mutations of the potential SD sequence and removal of the hairpin all decrease frameshifting as expected (see Extended Data Fig. 3, Fig. 4).

Elongation of the *dnaX* mRNA is drastically and abruptly perturbed at codon Lys7. Analysis of rates at each codon revealed a 10-fold increase in the rotated state (waiting for EF-G and translocation) lifetime (96 ± 18 s vs. 5~10 s for the other codons) at Lys7, corresponding to $tRNA^{Ala}(GCA_{21})$-codon pair in the ribosomal peptidyl-tRNA site (P site) and the newly incorporated $tRNA^{Lys}(AAA_{24})$ codon pair in the A site, poised for translocation; nonrotated state lifetimes (waiting for TC and peptide bond formation) remain constant at each codon (Fig. 1b, c, d). Furthermore by partitioning frameshifted vs. non-frameshifted ribosomes, an increased rotated-state lifetime at codon Lys7 is observed only for frameshifted ribosomes (138 ± 31 s); non-frameshifted ribosomes translate through the frameshift site seemingly unaffected (13 ± 4 s) (Fig. 1e, confirmed independently in Extended Data Fig. 2d, and repeated with varying factor concentrations in Extended Data Fig. 5). Disruption of the slippery sequence by changing A_{21} AAA_{24} AAG_{27} to G_{21} AAG_{24} AAG_{27} (A21GA24G mutant) caused an expected decrease in frameshifting efficiency to 12% (background level in our experiments is 3~10%), while drastically decreasing the lifetime at codon Lys7 (25 ± 5 s instead of 96 ± 18 s) (Extended Data Fig. 6). Thus, the long lifetime at codon Lys7 is a hallmark of frameshifting and requires the slippery-site sequence. Partitioning between frameshifted and non-frameshifted ribosomes was assumed to occur during the pause induced by frameshift signal. Instead, we demonstrate that the initial branch point occurs prior to the pause, but all frameshifted ribosomes exhibit a pause.

We next determined what is occurring during the pause that is characteristic of frameshifting. Normally translocation is coupled to ribosome reverse-rotation with deacylated tRNA in the ribosomal exit site (E site) departing rapidly after the ribosome reverse-rotates[16]. Using Cy3-labeled $tRNA^{Val}$, we observed E-site tRNA departure directly at the frameshift site on a GCA_{21} (Ala) to GUA_{21} (Val) mRNA mutant, without affecting the frameshifting behavior (Extended Data Fig. 7). We measured the departure of Cy3-$tRNA^{Val}$ relative to the Cy5-$tRNA^{Lys}$ arrival to the AAA_{24} (Lys7) codon in the A site, which defines the start of the long rotated-state pause, correlated to peptide bond formation and transition to the rotated state: departure of deacylated Cy3-$tRNA^{Val}$ relative to the arrival of Cy5-$tRNA^{Lys}$ at codon Lys7 estimates when and if translocation occurs during the pause. During translation of the *dnaX* mRNA, Cy3-$tRNA^{Val}$ departs on average 45 ± 11 s after the arrival of Cy5-$tRNA^{Lys}$ to the Lys7 codon (within photobleaching time of 196.7 ± 28.1 s). This time decreases with increasing concentration of EF-G, confirming that tRNA departure is linked to translocation (Fig. 2a). However, since the Cy3-$tRNA^{Val}$ residence time is much shorter than the rotated state lifetime (138 s), translocation occurs within the rotated state pause and precedes eventual reverse rotation. Thus translocation at Lys7 during frameshifting is uncoupled to reverse rotation of the ribosomal subunits. Translocation in this case is still inhibited through the interactions with the hairpin and internal-SD sequence, with time to translocation longer than normal translation.

Uncoupling of tRNA-mRNA translocation from reverse-rotation and E-site tRNA departure creates a non-canonical intermediate in translation: the ribosome has a peptidyl-tRNA in the P site, but remains in a rotated intersubunit conformation. What is the nature of this state and how is it linked to frameshifting? Is the A site available for tRNA binding in this state? To answer these questions, we correlated Cy5-$tRNA^{Lys}$ binding and departure events with the

intersubunit conformational FRET signal (Fig. 2b). Although the *dnaX* mRNA sequence consists of 4 Lys codons, 71% of elongating ribosomes exhibit >4 Cy5-Lys pulses (Fig. 2c) (equal to frameshifting percentage). The first three $tRNA^{Lys}$ pulses (Lys1, Lys5, and Lys7) show arrival rates and lifetimes consistent with elongation dynamics from intersubunit FRET data (Extended Data Fig. 8a, b); the third Lys7 pulse corresponds to the ribosome decoding AAA_{24} Lys7 at the slippery site (lifetime of 119.4 s, consistent with the rotated state lifetime at Lys7). The existence of the fourth and subsequent tRNA pulses directly indicate that translocation has occurred during the long rotated state and the A site is now available for aminoacyl-tRNA binding. After uncoupled translocation of the $tRNA^{Lys}$ to the P site, which would expose the fourth Lys codon (Lys8), $tRNA^{Lys}$ samples the A-site codon multiple times (on average ~2.3 times)[15], resulting in a buildup of Cy5 intensity (from two Cy5-$tRNA^{Lys}$ bound to the ribosome, Fig. 2b, c) even though the rotated state is not the natural substrate for tRNA binding to the A site. Mutation of the slippery sequence (A21GA24G) greatly suppresses additional sampling by Cy5-$tRNA^{Lys}$ (only 9.9% of elongating ribosomes exhibit > 4 pulses), indicating that multiple sampling events on Lys8 are characteristic of frameshifting and the long pause. Postsynchronization of the arrival of the 4^{th} sampling $tRNA^{Lys}$ to the time of uncoupled translocation shows that translocation gates the arrival of the sampling $tRNA^{Lys}$, confirming that $tRNA^{Lys}$ is indeed sampling the A-site codon exposed by translocation (Fig. 2d, Extended Data Fig. 8). Delivery of tRNA-EF-Tu-GDPNP (a non-hydrolyzable analog of GTP) instead of GTP decreases the tRNA pulse lifetimes from 38 ± 2 s to 2.1 ± 0.1 s, demonstrating that GTP hydrolysis by EF-Tu and subsequent accommodation of the tRNA into the ribosomal A-site occur for these long-lived sampling pulses.

What is the nature of the uncoupled translocation and how is it linked to $tRNA^{Lys}$ sampling to this non-canonical rotated state and to frameshifting[4,8,10]? We propose that uncoupled +3 translocation creates weakened codon-anticodon-ribosome interactions, and that $tRNA^{Lys}$-sampling and accommodation at the AAG_{27} codon presented by the non-canonical rotated ribosome drives the ribosome into the −1 frame and helps re-establish codon-anticodon interactions (see Extended Data Fig. 9). Consistent with this model, AAA_{26} (−1 frame) and AAG_{27} (0-frame) both encode Lys, but an AAG codon interacts less stably than an AAA codon with the UUU anticodon of Lys-$tRNA^{Lys}$ because of tRNA modifications and wobble pairing at the 3^{rd} position[19–21], favoring simultaneous slippage of the two codon-anticodon interactions in the −1 direction. Mutation of the AAG_{27} codon to AAA_{27} AAG(AAA) mutant removes this preference, correspondingly decreasing the frameshift percentage to 49%[19]. For the frameshifted ribosomes on the AAG(AAA) mutant, the characteristic long rotated-state stall (mean lifetime 126 ± 38 sec) is still observed, with $tRNA^{Lys}$ sampling driving to the −1 frame, as for the wild-type mRNA. However, there are two populations for the non-frameshifted ribosomes: one without the long pause (mean lifetime 8.3 ± 1.4 sec) where ribosomes translate unaffected through the frameshift site (as before), and a second new subpopulation with a long pause at codon Lys7 (mean lifetime 90.8 ± 18.6 sec) that remains in the 0 frame, with $tRNA^{Lys}$ sampling to the 0 frame (Fig. 2e). We also observe similar behavior when changing AAG_{27} to UUU_{27} (AAG(UUU)), eliminating possible slippage between the A-site and P-site tRNA-codon interactions, which decreases the frameshifting percentage to 20% (Fig. 2f). These results suggest that the long-lived rotated

state, with P-site tRNA and an empty A-site codon is not sufficient for frameshifting: there is an additional need for slippage between the A and P site tRNA codon-anticodon interactions. The final reading frame is established after uncoupled translocation, and that long-lived sampling of the A site by $tRNA^{Lys}$ serves to define reading frame before the non-canonical state can be resolved. Thus, there is a second branch point for reading frame determination during −1 frameshifting, which involves tRNA sampling in the A-site (Fig. 2g).

Once reading frame is established, how is the long-lived rotated state resolved to continue translation? We delivered Cy5-EF-G and correlated the EF-G pulses with the Cy3B/BHQ FRET signal (Fig. 3a). During the long rotated state, EF-G samples the ribosome multiple times[16] (on average >5 times per codon vs. ~1.3 per codon for non-frameshifting codons). Multiple long EF-G pulses (mean lifetime of ~ 1 sec vs. ~100 ms for non-frameshifting codons) are observed at codon 7. These are not observed if the slippery site is mutated; instead multiple short EF-G sampling events occur to allow translocation (Fig. 3b, c), consistent with an increased energy barrier imposed by the hairpin and SD interactions. For the wild-type mRNA, the long lifetime EF-G pulses occur most frequently during and after the uncoupled translocation (after ~40 seconds) (Fig. 3d), echoing a cryo-EM structure of a eukaroyotic ribosome over a −1 frameshifting signal in the rotated state showing that the eukaryotic equivalent of EF-G, eEF2, was trapped on the ribosome[9,22]. The long paused state is finally resolved by EF-G-GTP, as revealed by postsynchronization of ribosome reverse-rotation at the Lys7 codon correlated with occupancy of Cy5-EF-G (Fig. 3e). Thus, EF-G action resolves the frameshift state and resumes translation.

Here, we directly tracked translation in real time to follow the dynamics of frameshifting, developing a mechanistic model that embraces prior biochemical and structural studies[9,23]. We propose that the stochastic interaction of the ribosome with the hairpin helix in an open or closed state, and/or formation of the SD-antiSD pairing interaction represent the shunt to either pausing in the rotated state (which leads to uncoupled translocation) or normal translation[24]. The long-lived, rotated ribosomal state contains a peptidyl-$tRNA^{Lys}$ in the P-site and AAG_{27} codon in the A-site creating a non-canonical intermediate in translation, which is required for frameshifting and likely involves weakened tRNA-mRNA-ribosome contacts[25,26] and may involve hyper-rotation as recently proposed[27]. This state frustrates the normal action of both tRNA-EF-Tu -GTP and EF-G-GTP, accounting for the long pause. The repeated sampling of tRNAs to this state during the long pause allows the binding energy of the codon-anticodon pairing to be used to allow slippage while both P- and A-site tRNAs are on the ribosome and redefine the translational frame. Peptidyl-transfer is slow, since the rotated ribosome likely does not position the two tRNAs correctly for peptidyl transfer to occur efficiently. EF-G eventually resolves the state and continues translation. The competition between slow peptide-bond formation and slow translocation explains heterogeneous protein products in prior frameshifting studies[28] (Extended Data Fig. 10). Thus, frameshifting involves both EF-G and tRNA, and occurs at an unconventional point during elongation after translocation but before peptidyltransfer[11,29] (Fig. 4). The interplay of mRNA sequence and structure with ribosomal dynamics leads to branchpoints during elongation, creating non-canonical paused states that allow unusual events in elongation. Such states may be a central feature of translational control.

MATERIALS AND METHODS

Reagents and buffers for translation experiments

Escherichia coli ribosomal subunits and translation factors were prepared and purified as described before[37]. *E. coli* strain bearing hairpin loop extensions in phylogenetically-variable, surface-accessible loops of 16S rRNA in helix 44 and 23S rRNA in helix 101 were used to purify 70S ribosomes[38]. 30S and 50S subunits were prepared from dissociated 70S particles using previously described protocols[37]. 3′-dye labeled DNA oligonucleotides (labeled with Cy3B or BHQ-2) complementary to the mutant ribosome hairpins can then be used to label the ribosomes.

Translation factors (IF2, EF-Tu, EF-G, EF-Ts), S1, and fluorescently labeled Cy5-EF-G, were prepared as described previously for our single-molecule experiments[37,38,40]. A semi-purified mix of all aminoacyl-tRNA synthetases (aaRS) was prepared from *E. coli* S30 extract. Total or Δ(Lys, Val, Phe, or some combination) aminoacyl-tRNAs were prepared by incubating total *E. coli* tRNA (Sigma-Aldrich) with all amino acids (minus Lys, Val, Phe or some combination for Δ mixes) together with the aaRS mix for 30 min at 37°C in a buffer consisting of Tris-HCl (50 mM, pH 7.5), KCl (50 mM), $MgCl_2$ (10 mM), and β-ME (3 mM), complemented with ATP (2 mM), phosphoenol pyruvate (PEP, 10mM), pyruvate kinase (PK, 50 μg/ml), myokinase (MK, 2 μg/ml) and inorganic pyrophosphatase (PP_iase, 10 μg/ml). aa-tRNAs were thereafter purified by phenol extraction, ethanol precipitation, and gel filtration (Micro Bio-Spin Columns With Bio-Gel P-6 in Tris Buffer, Bio-Rad), and finally stored in small aliquots in −80°C.

E. coli $tRNA^{Phe}$, $tRNA^{Lys}$, and $tRNA^{Val}$ were purchased from Sigma-Aldrich. Phe-(Cy5)$tRNA^{Phe}$ and Lys-(Cy5)$tRNA^{Lys}$ were labeled with Cy5-NHS (GE Lifesciences) at acp^3U at position 47, purified as previously described[30], and aminoacylated as above. Val-(Cy3)$tRNA^{Val}$ was labeled with Cy3-maleimide (GE Lifesciences) at s^4U at position 8, purified and aminoacylated as above.

Synthetic biotinylated mRNAs were purchased from Dharmacon. All mRNAs had 5′-biotin followed by a 5'-UTR and Shine-Dalgarno sequence derived from gene 32 of the T4 phage (sequence described previously[18]), an AUG start codon, followed by the sequence of interest (as indicated in the figures).

All experiments were conducted in a Tris-based polymix buffer consisting of 50 mM Tris-acetate (pH 7.5), 100 mM potassium chloride, 5 mM ammonium acetate, 0.5 mM calcium acetate, 5 mM magnesium acetate, 0.5 mM EDTA, 5 mM putrescine-HCl and 1 mM spermidine. All single-molecule experiments had 4 mM GTP and were performed at 22°C.

Single-molecule experiments

3'-dye labeled DNA oligonucleotides (labeled with Cy3B or BHQ-2) complementary to the mutant ribosome hairpins[37,38] were ordered from Trilink. Right before each experiment, purified 30S and 50S ribosomal subunits (final concentration = 1 μM) were mixed in 1:1 ratio with the 3′ dye-labeled oligonucleotides specific for the hairpin extensions in each subunit for 37°C for 10 min and then at 30°C for 20 min in a Tris-based polymix buffer

system. 30S pre-initiation complexes (PICs) were formed as described[37] by incubating the following at 37 °C for 5 minutes: 0.25 μM Cy3B-30S, pre-incubated with stoichiometric S1, 1 μM IF2, 1 μM fMet-tRNA^{fMet}, 1 μM mRNA, and 4 mM GTP to form 30S PICs in the polymix buffer.

Before use, we pre-incubate a SMRT Cell V3 from Pacific Biosciences (Menlo Park, CA, USA), a zero-mode waveguide (ZMW) chip, with a 1 mg/ml Neutravidin solution in 50 mM Tris-acetate pH 7.5 and 50 mM KCl at room temperature for 5 minutes. The cell is then washed with Buffer 6 (50 mM Tris-acetate pH 7.5, 100 mM potassium chloride, 5 mM ammonium acetate, 0.5 mM calcium acetate, 5 mM magnesium acetate, and 0.5 mM EDTA). After washing, 40 μl of Buffer 6 is left in the cell to keep the cell surface wet. We then dilute the 30S PICs with our Tris-based polymix buffer containing 1 μM IF2 and 4 mM GTP down to 10 nM PIC concentration. The diluted PICs are then loaded into the SMRT cell at room temperature for 3 minutes to immobilize the 30S PICs into the ZMW wells. We wash away excessive unbound material with our Tris-based polymix buffer containing 1 μM IF2, 4 mM GTP, 1 mM Trolox, and a PCA/PCD oxygen scavenging system (2.5 mM 3,4-dihydroxybenzoic acid and 250 nM protocatechuate deoxygenase[43]). After washing, 20 μl of the fresh washing mix were added to the cell to keep the surface wet and to prevent exposure of the immobilized dye labeled biomolecules to oxygen.

We formed ternary complexes (TCs) between total charged *E. coli* tRNAs and EF-Tu(GTP) as described[37]. Total or Δ(aa) aminoacyl-tRNA·EF-Tu·GTP ternary complexes were pre-formed by incubating (2 min at 37C) the aa-tRNAs with five-fold excess of EF-Tu, GTP (1 mM), PEP (3 mM) and EF-Ts (40 μM) in polymix. The ternary complexes (1 ~ 6 μM) were added to BHQ-50S (200 nM), EF-G (80 ~ 480 nM), IF2 (1 μM), GTP (4 mM), 2.5 mM Trolox, and the oxygen scavenging system (PCA/PCD) to form a delivery mix in polymix buffer. Many of the experiments are done at 1 μM ternary complexes and 80 nM EF-G (chosen to have well-defined, detectable FRET transition signals), unless indicated otherwise.

Before starting an experiment, the SMRT Cell is loaded into a modified PacBio RS sequencer[14]. At the start of the elongation experiment, the instrument illuminates the SMRT cell with a green laser and then delivers 20 μl of a delivery mixture onto the cell surface at *t* ~ 10 sec.

Translation experiments with labeled tRNAs

Translation experiments using labeled tRNAs are performed in the same way as ribosome Cy3B/BHQ conformational FRET experiments with the following differences. Total tRNA mixture was charged with all amino acids except the tRNA amino acid we wish to observe. The resulting mix of all charged tRNAs except tRNA of interest that remains uncharged was used to form ternary complexes. Ternary complexes with the labeled tRNA are separately formed. For example, we will form a ternary complex with Phe-(Cy5)tRNA^{Phe} and Δ(Phe) aa-tRNA. The delivery mix contains: 200 nM BHQ-50S, 1 μM IF2, 80~320 nM EF-G, 1~3 μM total tRNA Δaa ternary complexes, 200 nM aa-(Cy3/Cy5)tRNA^{aa} ternary complexes, 4 mM GTP, 1 mM Trolox, and the PCA/PCD oxygen scavenging system in the Tris-based polymix buffer. All experiments are performed at 200 nM labeled-tRNA ternary complexes.

During the experiment, the SMRT Cell is illuminated with both a green and a red laser. The experiments involving tRNA transit of Cy3-tRNA^{Val} (200 nM) and Cy5-tRNA^{Lys} (200 nM) are done the same way, except the ribosomes were not labeled and a ΔValΔLys aa-tRNA (3 μM) mixture is used with 80 ~ 320 nM EF-G.

Correlation experiments with Cy5-EF-G

Cross-correlation experiments between our ribosome Cy3B/BHQ conformational FRET signal and our EF-G binding signal are conducted exactly as above but with a different delivery mix and laser illumination. The delivery mix for the cross-correlation experiment contains: 200 nM BHQ2–50S, 1 μM IF2, 80 ~ 240 nM Cy5-EF-G, 1 ~ 3 μM total tRNA ternary complexes, 4 mM GTP, 1 mM Trolox, and the PCA/PCD oxygen scavenging system in Tris-based polymix buffer. The data presented in Figure 4 are performed at 80 nM Cy5-EF-G and 1 μM total tRNA ternary complexes. Dual illumination of SMRT Cell with a green and a red laser are used.

ZMW instrumentation and data analysis

All single-molecule fluorescence experiments were conducted using a commercial PacBio RS sequencer that we modified to allow the collection of single-molecule fluorescence intensities from individual ZMW wells about 130 nm in diameter in 4 different dye channels corresponding to Cy3, Cy3.5, Cy5, and Cy5.5[14]. The RS sequencer has two lasers for dye excitation at 532 nm and 632 nm. In all experiments, data was collected at 10 frames per second (100 ms exposure time) for 8 minutes. The energy flux of the green laser is 0.48 μW/μm^2 and the red laser is at 0.22 μW/μm^2.

Data analyses for all experiments are conducted with MATLAB (MathWorks) scripts written in-house[16]. Briefly, traces from the ZMW wells are initially selected based on fluorescence intensity, fluorescence lifetime, and the changes in intensity. Filtered traces exhibiting intersubunit FRET or single-molecule binding signals are then selected for further data analysis. The FRET states are assigned as previously described based on a hidden Markov model based approach and visually corrected[18]. All lifetimes were fitted to a single-exponential distribution using maximum-likelihood parameter estimation in MATLAB.

Extended Data

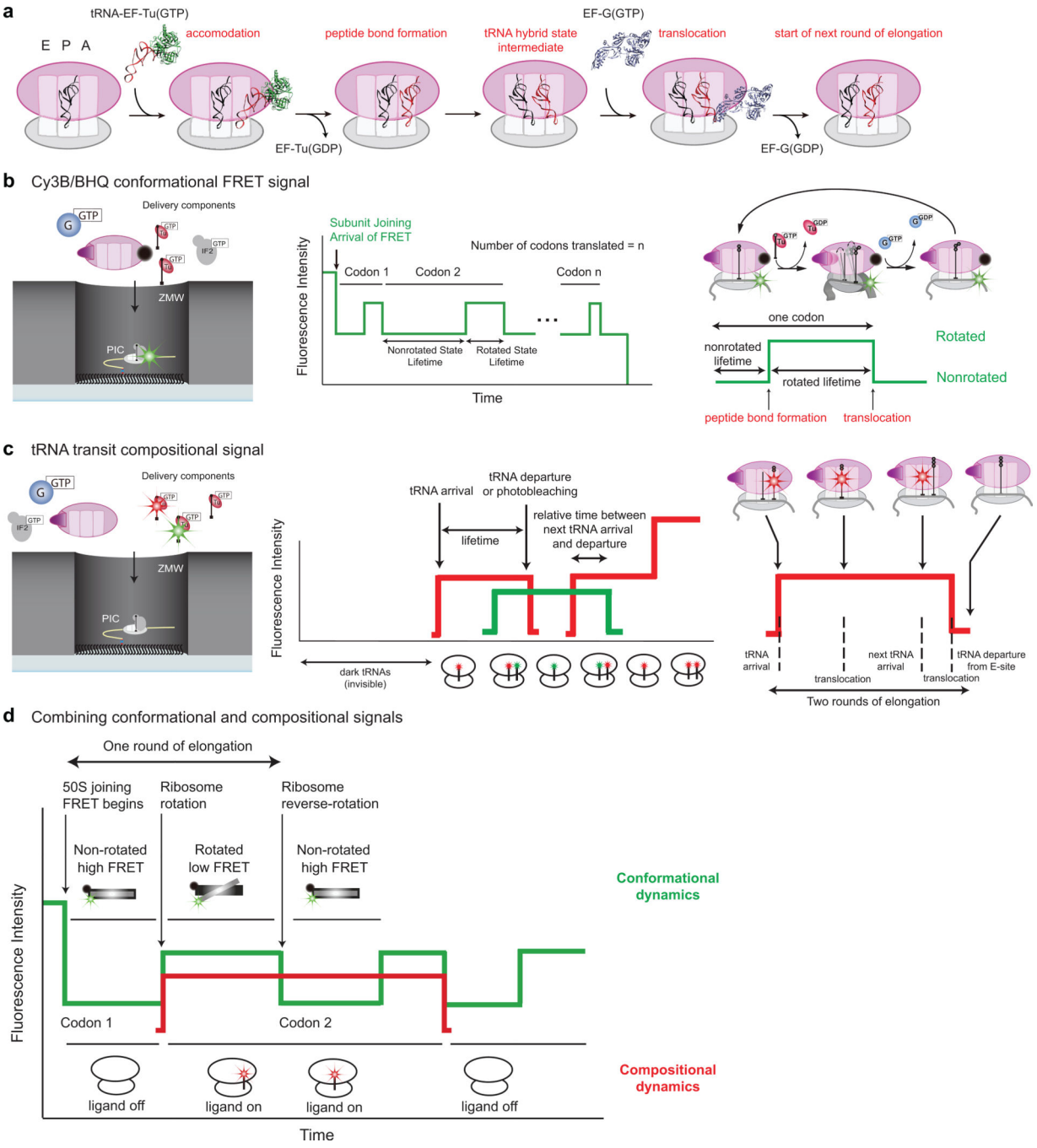

Extended Data Figure 1. Explanation and schematics of the experimental signals

(a) Different stages of the elongation cycle during translation. Frameshifting have been proposed to occur at each of the steps: (1) during accommodation of the A-site tRNA[4], (2) subsequent to accommodation, but prior to peptide bond formation[8], (3) during tRNA hybrid-state intermediates[10], (4) during translocation[9], and (5) at the start of the next found of elongation[11].

(b) The ribosome starts each round of elongation in the nonrotated state. In this "locked" state, the P-site tRNA is stably bound in the classical state, preserving the reading frame of the mRNA[18]. Upon A-site tRNA selection and peptide bond formation, the 30S subunit rotates 3~10° counterclockwise with respect to the 50S subunit to the rotated state (pre-translocation)[26,31,32]. This "unlocked" state permits tRNA motions and the tRNA can fluctuate freely between the classical state and hybrid state[33], thus facilitating translocation of tRNA and movement of ribosome by one codon over mRNA[34,35]. Peptide-bond formation also triggers spontaneous fluctuations of the L1 stalk between open and closed conformations as well as spontaneous rotations in ribosome conformations[32,36]. EF-G then catalyzes translocation, and the ribosome returns to the nonrotated state (post-translocation). To monitor the rotational state of the ribosome in real time, we employed FRET between the small (30S) and large (50S) subunits. The 30S subunit was site-specifically labeled with Cy3B on helix 44, and a nonfluorescent quencher, BHQ-2, was placed on helix 101 of 50S subunit[18,37,38]. Reagent delivery of BHQ-50S, tRNA ternary complex, and EF-G to surface immobilized Cy3B-30S pre-initiation complexes in ZMWs results in IF2-guided 70S assembly during initiation and establishment of FRET between the two ribosomal subunits: upon subunit joining[39], the green (Cy3B) intensity drops, which is followed by alternating low-high-low intensities Each alternating cycle corresponds to the ribosome translating a single codon, with the two intensity states consistent with the two rotational states of the ribosome: the low intensity state (high FRET) defining the nonrotated (locked) ribosome conformation and the high intensity state (low FRET) the rotated (unlocked) conformation[18]. The rotated- and nonrotated-state lifetimes at each codon can be statistically analyzed.

(c) During each cycle of elongation, the ribosome selects the aminoacyl-tRNA in a ternary complex with EF-Tu-GTP, and positions the tRNA in the A site. Upon A-site tRNA accommodation, the ribosome rapidly catalyzes peptide bond formation with the P-site tRNA[34,40]. Translocation moves A- and P-site tRNA-mRNA complexes to the E and P site respectively, catalyzed by the EF-G. The compositional dynamics of tRNA and EF-G on the ribosome, here defined as the relative timing of their arrival and departure during elongation, can be observed by labeling the tRNA or EF-G with Cy3 or Cy5. Cy5/Cy3-tRNA arrival to the surface immobilized ribosomes is marked by a red/green fluorescent pulse. Translation can be monitored by the arrival and departure of dye-labeled tRNA. Each productive tRNA binding event results in a fluorescence pulse that lasts as a ribosome translates 2 codons – beginning with arrival of tRNA in the A-site, continuing through tRNA translocation to the P-site, arrival of A-site tRNA to the next codon, a second round of translocation, and ending with spontaneous dissociation of tRNA from the E site[30]. To track tRNA and EF-G dynamics on translating ribosomes at near-physiological concentrations of fluorescent factors (0.1 – 1 μM), we used ZMWs to detect hundreds of individual ribosomes[30]

(d) Substituting the traditional FRET acceptor, Cy5, with BHQ-2 allowed the use of Cy5 to label other translation components for correlation studies. The Cy3B intensity reports on the conformational state of the ribosome, while Cy5 pulses indicate arrival, occupancy, and departure of ribosomal ligands.

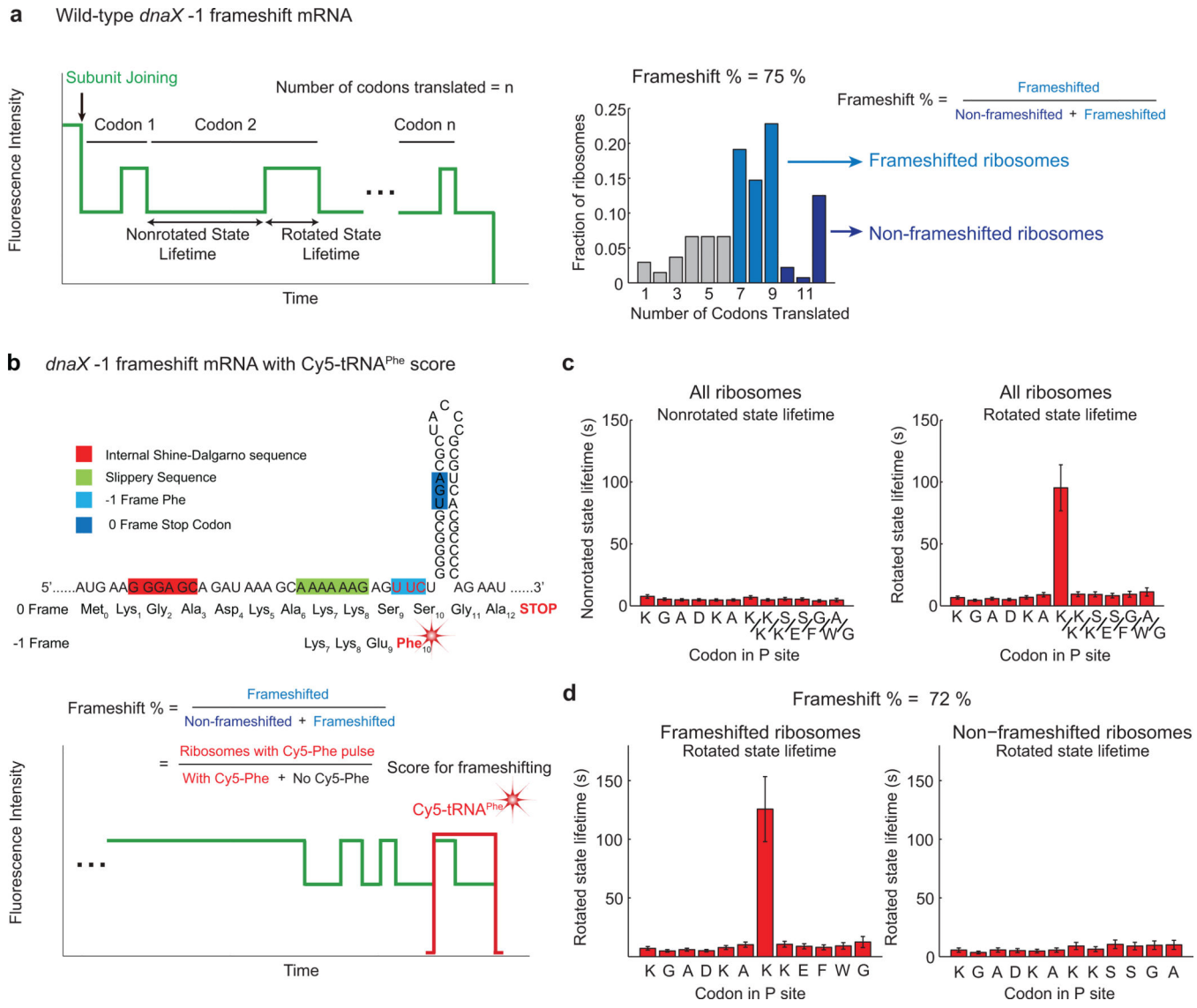

Extended Data Figure 2. Phe codon in the −1 frame confirms the characteristic long pause during frameshifting

(a) Histogram of the fraction of ribosomes translating to a particular codon for the *dnaX* −1 frameshift mRNA, with a schematic. Many of the ribosomes translate up to 12 codons where the 0 frame stop codon is, though a large percentage of ribosomes translate up to 9 codons, where the −1 frame stop codon is. There are also ribosomes that stall at codon 7, limited by Cy3B photobleaching or end of movie (8 minutes) from the long rotated state pause. Interestingly, there are also a significant number of ribosomes that stall at codon 8 (see Extended Data Fig. 10 for discussion). By parsing the number of ribosomes that translate beyond codon 9 and up to codon 9, the frameshifting percentage can be calculated (75%). However, since non-frameshifted ribosomes may terminate early, this would lead to a slight over-estimate of the frameshifting percentage (3~10%). The frameshifting efficiency has been independently confirmed using a Cy5-tRNA^{Phe} score, as described below. Number of molecules analyzed n = 256.

(b) A UUC(Phe) codon is introduced in the −1 frame downstream of the slippery site. Frameshifting can be scored by an appearance of a Cy5 (red) pulse with Cy5-tRNA^{Phe} in addition to the Cy3B/BHQ conformational FRET signal. This allows us to independently score for frameshifting.

(c) Using the Cy5-tRNA^{Phe} as a score to confirm frameshifting, we get the same dynamics and lifetimes: the nonrotated state lifetimes remain constant at each codon, and the rotated state lifetime increases 10-fold at codon Lys7 at the slippery sequence. This confirms and justifies our results in Figure 1. Number of molecules analyzed n = 474. Error bars, s.e.

(d) By using the Cy5-tRNA^{Phe} as a score, we can parse the rotated state lifetimes into ribosomes that frameshifted and ribosomes that did not frameshift. We also get the same results as Figure 1: non-frameshifted ribosomes translate through the frameshift sequence seemingly unaffected; frameshifted ribosomes exhibit the characteristic long-rotated state pause at codon Lys7. Number of molecules analyzed n = 474. Error bars, s.e.

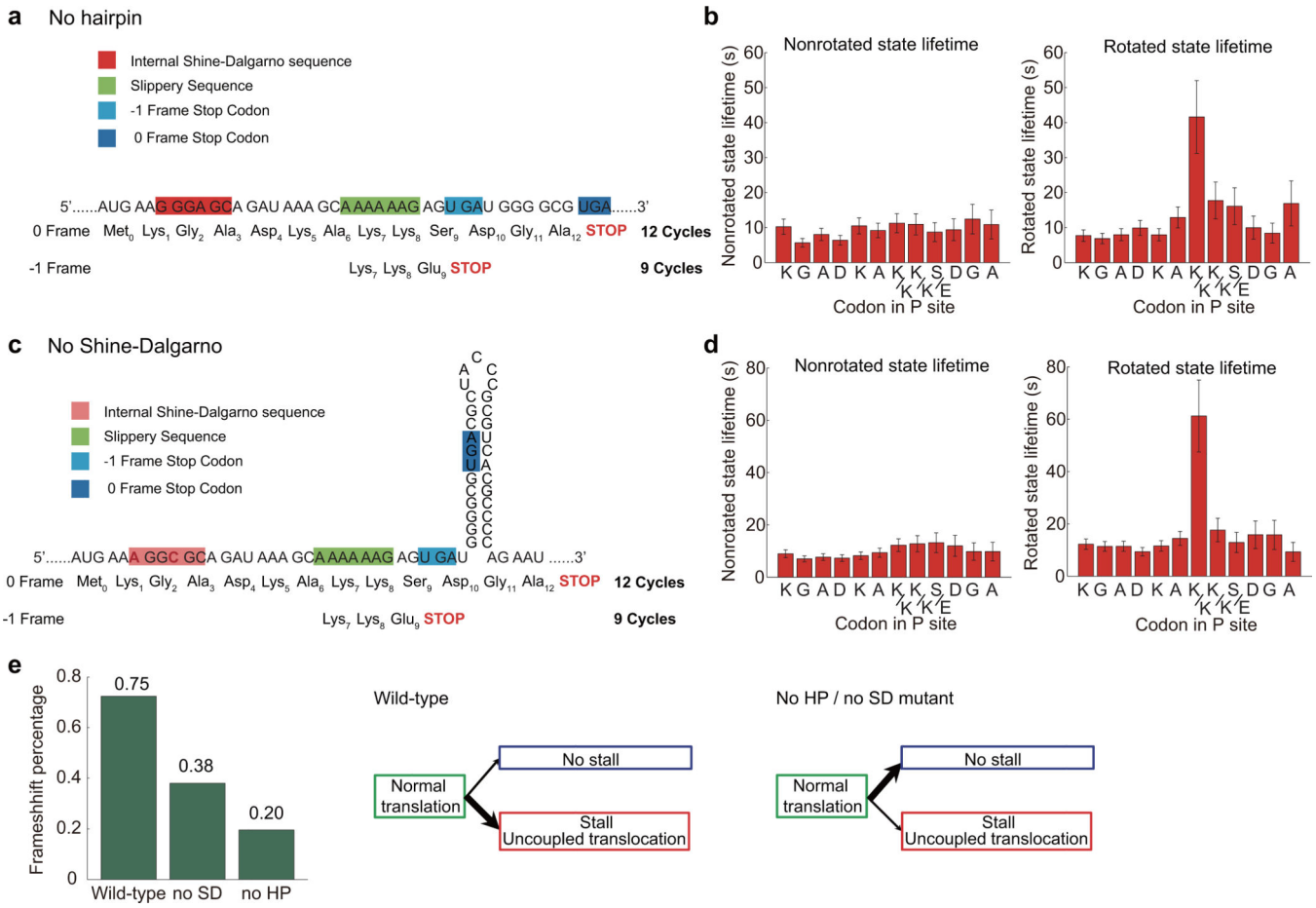

Extended Data Figure 3. Hairpin and the internal Shine-Dalgarno sequence are important for frameshifting

(a) mRNA sequence of the no hairpin (no HP) mutant. The mRNA consists of the same sequence as the wild-type *dnaX* frameshift sequence, but with the sequence after the UGA stop codon in the 0 frame in the hairpin deleted.

(b) Nonrotated and rotated state lifetimes in the presence of 80 nM EF-G and 1 μM $tRNA_{tot}$. The nonrotated state lifetimes are constant at each codon. There is an increase in rotated state lifetime at codon Lys7. Number of molecules n = 124. Error bars, s.e.

(c) mRNA sequence of the no Shine-Dalgarno (no SD) mutant. The mRNA consists of the same sequence as the wild-type *dnaX* frameshift sequence, but with the original internal Shine-Dalgarno sequence GGGAGC mutated to AGGCGC, decreasing the rRNA-mRNA interaction energy from −3.00 kJ/mol to −0.06 kJ/mol.

(d) Nonrotated and rotated state lifetimes in the presence of 80 nM EF-G and 1 μM $tRNA_{tot}$. The nonrotated state life is constant. There is an increase in rotated state lifetime at codon Lys7. Number of molecules n = 225. Error bars, s.e.

(e) Frameshifting percentages of the no SD and no HP mutant. Without the Shine-Dalgarno sequence, frameshifting percentage drops by half. Without the hairpin, frameshifting percentage drops to a quarter of the wild-type sequence. This indicates that both the internal Shine-Dalgarno sequence and the hairpin are required for efficient frameshifting, confirming that the hairpin and internal SD are stimulatory elements for frameshifting. These stimulatory elements may present a barrier and tension to translocation that is a prerequisite for efficient frameshifting.

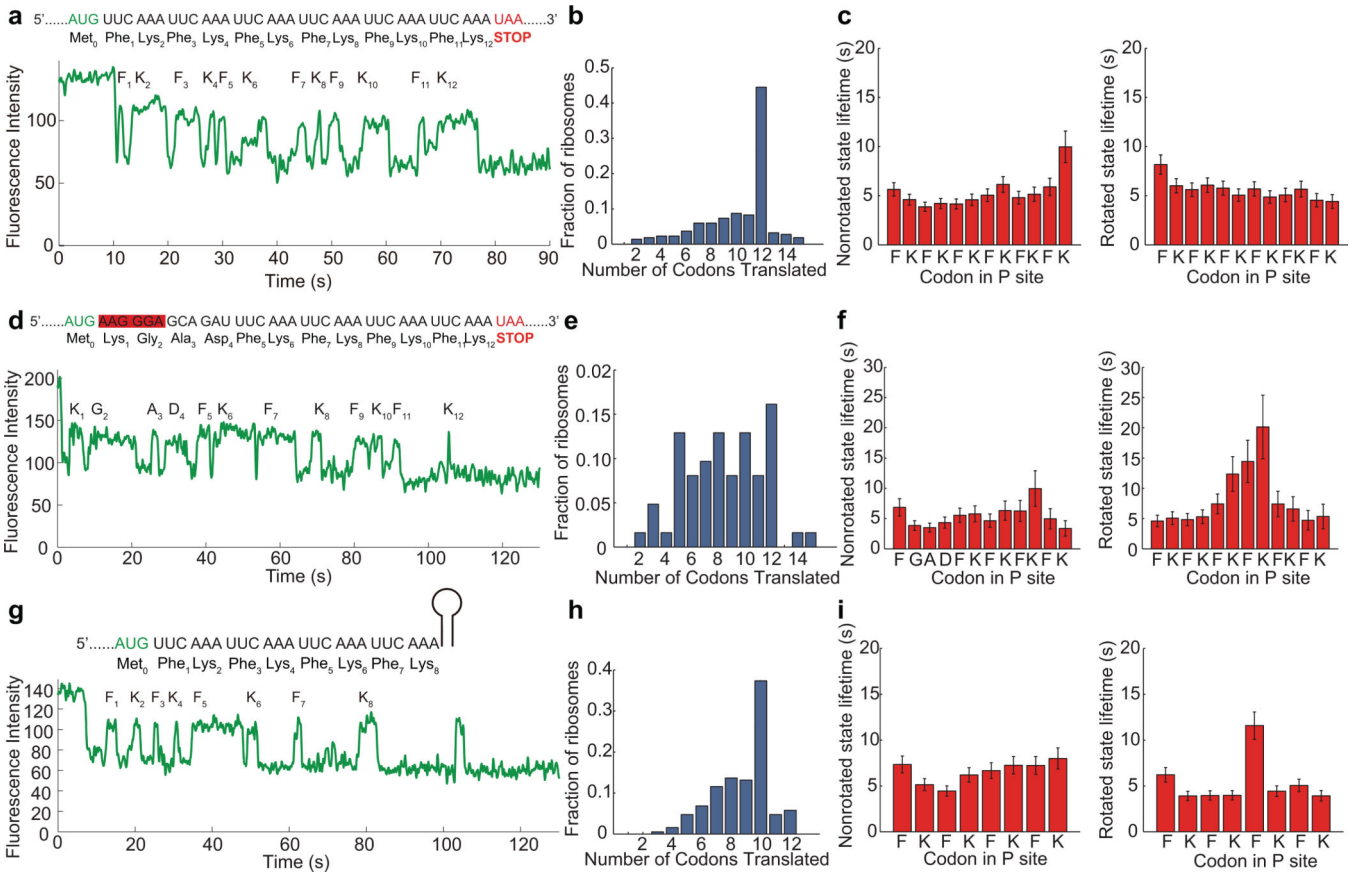

Extended Data Figure 4. Hairpin and internal Shine-Dalgarno sequences increases the energy barrier to translocation

(a) Translation of a short linear mRNA, 6(FK), in the presence of 80 nM EF-G and 1 μM $tRNA_{tot}$, with an example trace.
(b) Histogram of fraction of ribosomes translating to a particular codon. Most of the ribosomes translate up to 12 codons. Ribosomes translate <12 codons are due to photobleaching of the Cy3B dye, or non-processive ribosomes. This gives us a background level of 3~10% for our frameshifting efficiency analysis. The small number of ribosomes that translate beyond codon 12 are likely errors in our statistical analysis or read-through of the stop codon. Number of molecules analyzed n = 462.
(c) Rotated and nonrotated state lifetimes are fairly constant. Number of molecules analyzed n = 462. Error bars, s.e.
(d) Translation of a Phe-Lys sequence preceded by an internal Shine-Dalgarno sequence (same SD sequence used in the *dnaX* frameshift mRNA of this study) in the presence of 80 nM EF-G and 1 μM $tRNA_{tot}$, with an example trace.
(e) Histogram of fraction of ribosomes translating to a particular codon. Number of molecules analyzed n = 60.
(f) There is an increase in rotated state lifetime at codon 5 ~ 7. There is an increase in the rotated state lifetimes 3~4 fold over 3~5 codons downstream of the SD-like sequence, while the non-rotated state lifetime remains unaffected. The internal SD-like sequences may base pair with the 3' end of the 16S rRNA and slow down ribosomes in the pre-translocation state, echoing several work done previously by tracking ribosome movement and ribosome profiling[41,42]. Number of molecules analyzed n = 60. Error bars, s.e.
(g) Translation of a Phe-Lys sequence followed by a hairpin (same hairpin used in the *dnaX* frameshift mRNA of this study) in the presence of 80 nM EF-G and 1 μM $tRNA_{tot}$, with an example trace.
(h) Histogram of fraction of ribosomes translating to a particular codon. Number of molecules analyzed n = 332.
(i) Nonrotated state lifetimes are fairly constant. There is an increase in rotated state lifetime at codon 5, exactly 3 codons before the start of the hairpin, placing the ribosome directly at the first encounter of the hairpin. The relative position also matches where we see the long-rotated state pause during frameshift. This echoes the work done by Tinoco *et al*. where they showed the ribosome is capable of translating through the secondary structure through two mechanisms: ribosome translocating when encountering an open-state junction, occurring naturally or induced by the ribosome, or mechanically unwinding by the ribosome when encountering a closed-state junction[24]. When the ribosome encounters an open-state junction, translation proceeds at a constant rate; however, when a closed-state junction is encountered, the ribosome actively unwinds the secondary structure, resulting in a slight waiting time for translocation, after which the hairpin is biased by the ribosome into an open-state and translation occurs normally. The shunt to either pausing in the rotated state (which leads to uncoupled translocation) or normal translation during frameshifting is likely due to this mechanism. Number of molecules analyzed n = 332. Error bars, s.e.

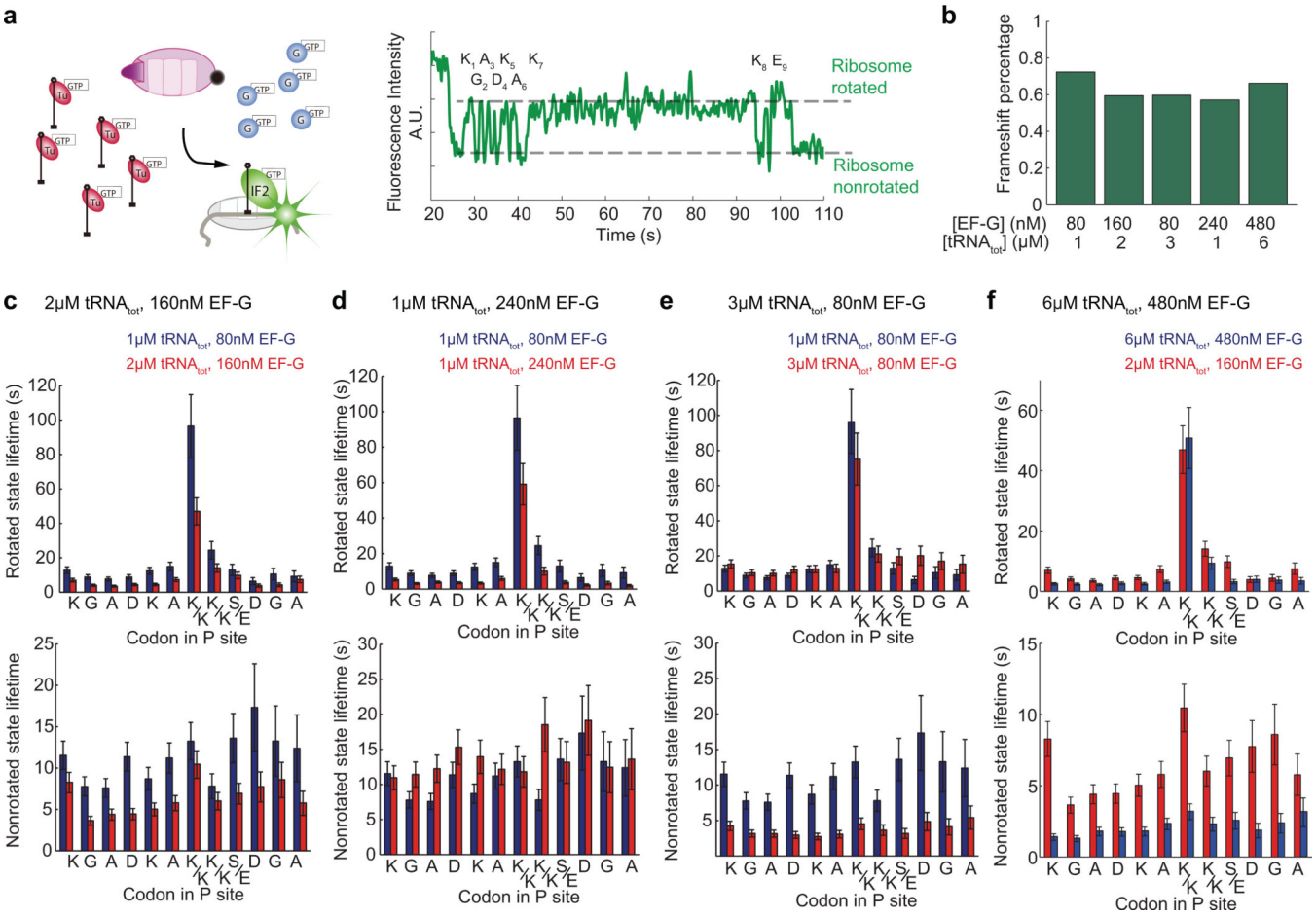

Extended Data Figure 5. Dynamics of frameshifting at different factor concentrations

(a) Example trace and schematic of a ribosome translating the *dnaX* frameshift mRNA at much higher factor concentrations (6 μM $tRNA_{tot}$ and 480 nM EF-G).

(b) Frameshifting efficiency does not depend on EF-G and $tRNA_{tot}$ concentrations.

(c) Increasing the $tRNA_{tot}$ and EF-G concentrations two-fold (from 1 μM $tRNA_{tot}$ and 80 nM EF-G to 2 μM $tRNA_{tot}$ and 160 nM EF-G) decreases both the rotated state lifetime and nonrotated state lifetimes. This confirms that our conformational FRET signal depends correctly on factor concentration. The lifetime of the long rotated state pause at codon Lys7 is also decreased by half, indicating that EF-G and/or tRNA interacts with the ribosome in that state. Number of molecules analyzed $n = 256$, $n = 234$. Error bars, s.e.

(d) Increasing the $tRNA_{tot}$ concentration (from 1 μM to 3 μM) while keeping EF-G concentrations constant decrease the non-rotated state lifetimes 3-fold as expected. The rotated state lifetimes remain the same except for codon Lys7; this is expected because the rotated state lifetime depends only on concentration of EF-G. Unexpectedly, the rotated state lifetime at codon Lys7 is also slightly decreased, suggesting a linkage between tRNA and EF-G dynamics at that long rotated-state stall. This echoes our results in Figure 2 that tRNA ($tRNA^{Lys}$ in this case) samples the uncoupled rotated-state after translocation, and the tRNA sampling and accommodation may help to re-establish the ribosome's reading frame and reverse-rotate subsequently. Thus, increasing tRNA concentrations (especially $tRNA^{Lys}$ in

this case) will decrease the long rotated-state lifetime. Number of molecules analyzed n = 526. Error bars, s.e.

(e) Increasing the EF-G concentration (from 80 nM to 240 nM) while keeping $tRNA_{tot}$ concentration constant decreases the rotated state lifetime 3-fold. The nonrotated state lifetime, which depends on the tRNA concentration, remains the same. However, the decrease in the rotated lifetime at codon Lys7 is only around 2-fold, rather than 3-fold as expected. This echoes our result in Figure 2 as well as part (b) above, suggesting that tRNA sampling also plays a role at this codon. Number of molecules analyzed n = 314. Error bars, s.e.

(f) Increasing the EF-G and $tRNA_{tot}$ concentrations further to 6 μM $tRNA_{tot}$ and 480 nM EF-G further decreases the rotated and nonrotated state lifetimes. However, the rotated state lifetime at codon Lys7 remains the same when compared with 2 μM $tRNA_{tot}$ and 160 nM EF-G. The long $tRNA^{Lys}$ sampling events observed in Figure 2 may be contributing to the long rotated state lifetime at codon Lys7.

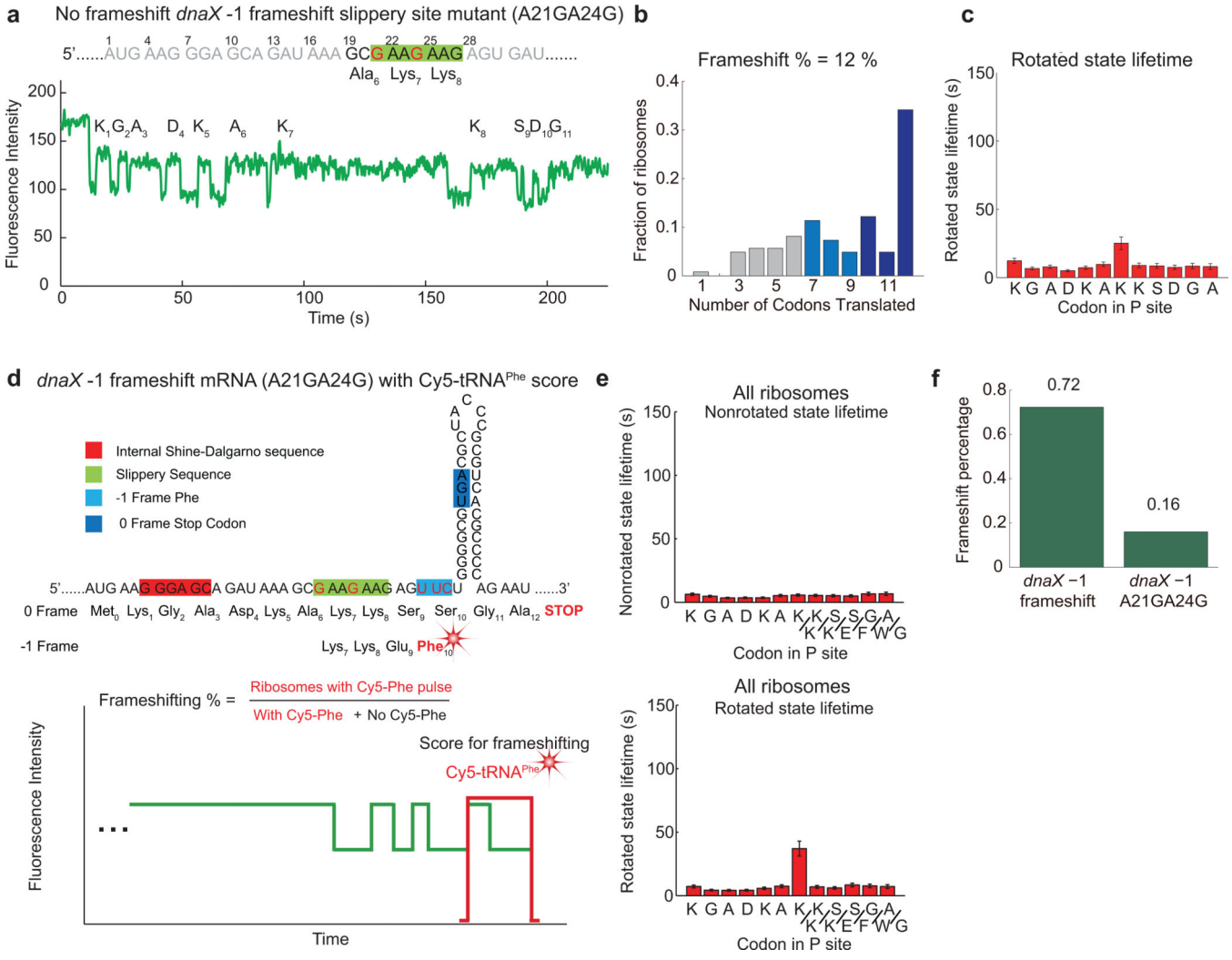

Extended Data Figure 6. Slippery sequence mutation (A21GA24G) decreases frameshifting percentage

(a) Example trace of a ribosome translating the A21GA24G mutant mRNA in the presence of 80 nM EF-G and 1 μM $tRNA_{tot}$. There seems to be a slightly longer pause at codon Lys7.
(b) Histogram of the fraction of ribosomes translating to a particular codon for the *dnaX* −1 frameshift A21GA24G mRNA. Most of the ribosomes translate up to 12 codons where the 0 frame stop codon is. The buildup of ribosomes stalled at codon 9 present during frameshifting disappears. By parsing the number of ribosomes that translate beyond codon 9 and up to codon 9, the frameshifting percentage can be calculated (12%).
(c) The rotated-state lifetime. The long stall at Lys7 is decreased with the slippery site mutant, suggesting that the extra-long pause is indeed a result of frameshifting. The slight increase in lifetime at Lys7 is due to the effects of the hairpin and internal Shine-Dalgarno sequence. Number of molecules analyzed $n = 230$. Error bars, s.e.
(d) A UUC(Phe) is introduced in the −1 frame downstream of the slippery site of the A21GA24G mutant, similar to above. The A21GA24G mutation is known to decrease frameshifting efficiency down to background levels[19].
(e) The nonrotated state lifetime and rotated-state lifetime match with our results using codon counting (see above). In the absence of frameshifting, there is still an increase in rotated state lifetime at codon Lys7, due to the increased energy barrier to translocation by the hairpin and internal Shine-Dalgarno sequence, though this increased lifetime is still much less than the Lys7 rotated state lifetime during frameshifting. Number of molecules analyzed $n = 538$. Error bars, s.e.
(f) Using Cy5-$tRNA^{Phe}$ as a score for frameshifting, frameshifting percentage matches with our previous results. The slippery sequence A21GA24G mutant decreases frameshifting percentage down to background levels. Number of molecules analyzed $n = 474$, $n = 538$.

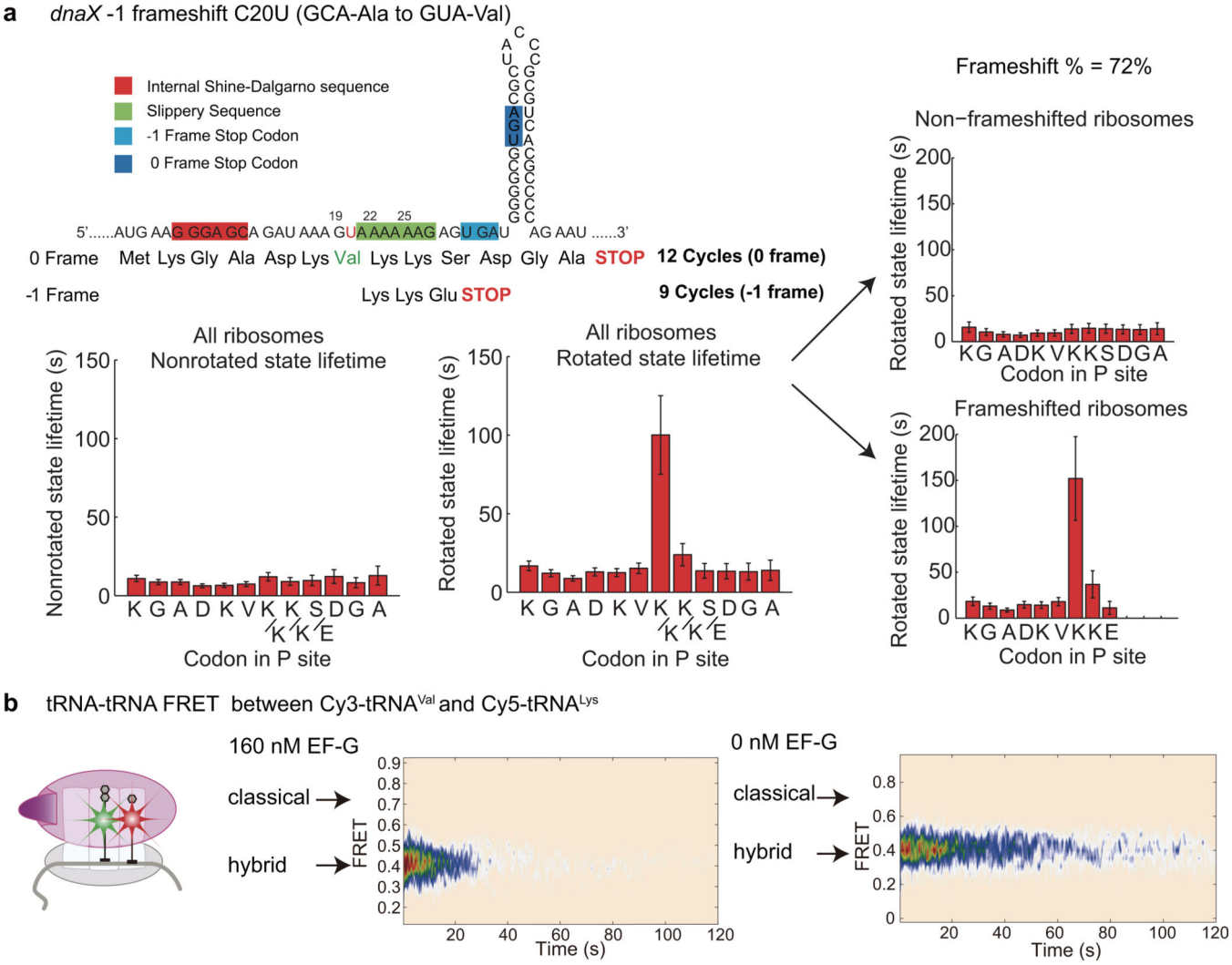

Extended Data Figure 7. tRNA dynamics during frameshifting with the *dnaX* GCA(Ala) to GUA(Val) mutant mRNA

(a) The 3 nucleotides upstream of the slippery sequence (GCA(Ala)) is mutated to GUA(Val) (named the C20U mutant) so that E-site tRNA dynamics can be observed during frameshifting since $tRNA^{Val}$ can be labeled with Cy3-maleimide (see Figure 2). This allows us to estimate the time to translocation during the long rotated-state pause at codon Lys7, since translocation of the Cy3-$tRNA^{Val}$ from the P-site to the E-site leads to rapid departure of the $tRNA^{Val}$ and disappearance of the Cy3 signal. We want to make sure that the C20U mutation does not affect frameshifting dynamics. The nonrotated state and rotated state lifetimes, as well as frameshifting percentages, are consistent with what we have observed before for the wild-type sequence. Number of molecules analyzed n = 266. Error bars, s.e. (b) tRNA-tRNA FRET between the Cy3-$tRNA^{Val}$ in the P site and the incoming Cy5-$tRNA^{Lys}$ at Lys7 in the A site at the slippery sequence. The tRNAs are in a hybrid state upon encountering of hairpin and engagement with the internal Shine-Dalgarno sequence. After translocation, the Cy3-$tRNA^{Val}$ departs from the ribosome, resulting in a disappearance of FRET. After translocation and uncoupling with ribosome reverse-rotation,

the now P-site tRNA^{Lys} is likely in a hybrid, or "distorted" conformation, according to the structure by Namy *et al*[9]. Number of molecules analyzed, top *n* = 227, bottom *n* = 337.

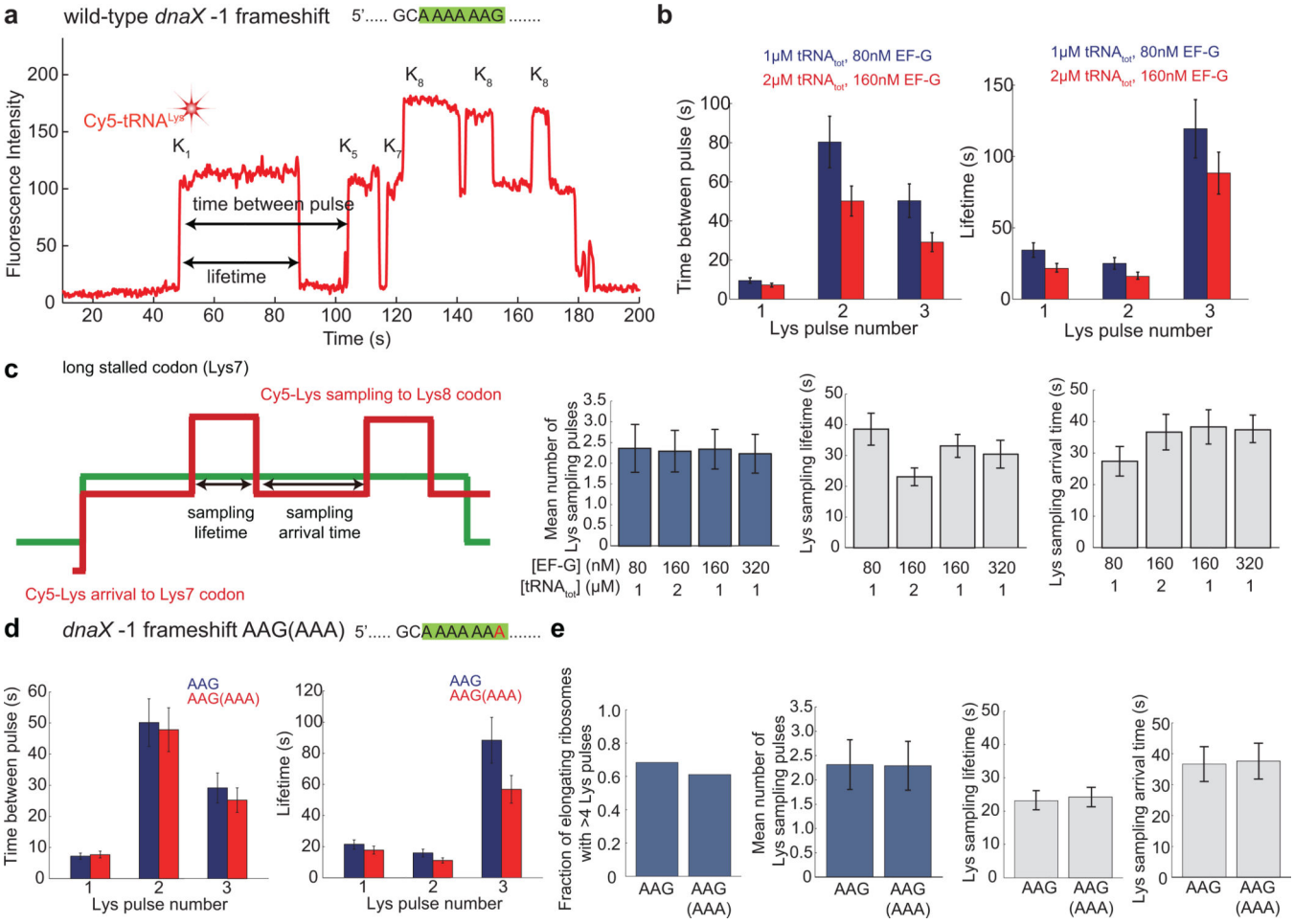

Extended Data Figure 8. tRNA^{Lys} transit and sampling dynamics

(a) Example trace of Cy5-tRNA^{Lys} transit during translation of the *dnaX* frameshift mRNA, indicating the definition of pulse lifetime and time between pulse.

(b) The time between tRNA^{Lys} pulse and lifetime of each pulse for the first three Lys codons are consistent with what is expected, and decrease expectedly with the increase of EF-G concentration and tRNA$_{total}$(ΔLys) concentration ([Cy5-tRNA^{Lys}]= 200 nM). The time between pulse for the first Lys pulse corresponds to the decoding of the first codon Lys1 of the mRNA after 50S subunit joining to the immobilized 30S, which is short as expected and does not depend on factor concentration. The second Lys pulse has a longer time between pulse, corresponding to the ribosome translating four codons from Lys1 to Lys5. The third pulse has a slightly shorter time between pulse, corresponding to the ribosome translating from codon Lys5 to Lys7. The lifetimes for the first two pulses are short, since the ribosomes decode and translocate the corresponding codons normally. The lifetime for the third pulse at codon Lys7 is long, corresponding to the ribosome at the long rotated-state pause during frameshifting. Number of molecules analyzed, *n* = 179 and *n* = 212. Error bars, s.e.

(c) Mean number of additional $tRNA^{Lys}$ sampling pulses to the long rotated-state pause at codon Lys7, sampling lifetimes, and sampling arrival times, at various concentrations of EF-G and $tRNA_{tot}$ ([Cy5-$tRNA^{Lys}$] = 200 nM) for ribosomes translating the *dnaX* −1 wild-type frameshifting sequence. There is a mean number of ~2.3 sampling $tRNA^{Lys}$ pulses, which remains constant at the various factor concentrations. There seems to be an interplay (competition) between EF-G and the other tRNAs on $tRNA^{Lys}$ sampling. Increasing the concentration of other factors increase the arrival time for $tRNA^{Lys}$, probably because they are all competing for the ribosomal A site. Number of molecules analyzed, from left to right, n = 179, n = 212, n = 180, n = 162. Error bars, s.e.

(d) The time between $tRNA^{Lys}$ pulse and lifetime of each pulse for the first three Lys codons are the same for the wild-type AAG sequence and the AAG(AAA) mutant sequence. Number of molecules analyzed n = 212 and n = 454. Error bars, s.e.

(e) By translating the AAG(AAA) mutant in the presence of Cy5-$tRNA^{Lys}$, we see similar dynamics as the *dnaX* wild-type sequence. Cy5-$tRNA^{Lys}$ samples the A site at codon Lys8 after uncoupled translocation at the frameshift site. The fraction of ribosomes exhibiting >4 $tRNA^{Lys}$ pulses are the same for the wild-type sequence and the AAG(AAA) mutant. The mean number of $tRNA^{Lys}$ sampling pulses, the mean arrival time, and the mean lifetimes of the sampling pulses to the long rotated-state stall are the same for the AAG(AAA) mutant and the *dnaX* wild-type sequence. Number of molecules analyzed, n = 212, n = 454. Error bars, s.e.

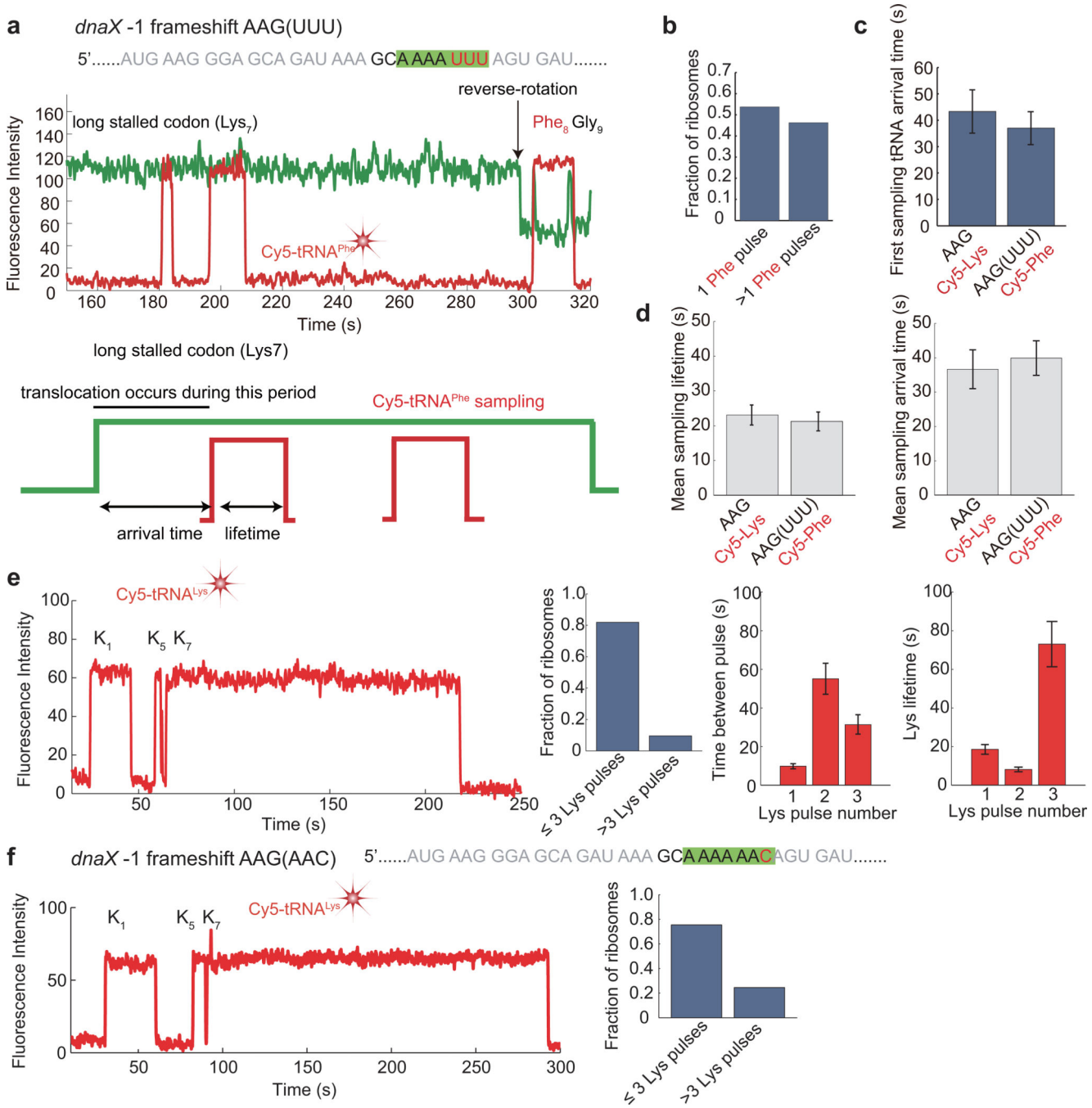

Extended Data Figure 9. tRNA sampling dynamics and slippage during frameshifting

(a) Example traces of Cy5-tRNA^{Phe} (red) sampling to the A-site Phe8 codon during the long rotated-state pause correlated with Cy3B/BHQ conformational FRET signal (green) for the AAG(UUU) mutant.

(b) By translating the AAG(UUU) mutant in the presence of Cy5-tRNA^{Phe} (red) and correlating with the Cy3B/BHQ conformational FRET signal (green), we can observe the fraction of ribosomes exhibiting only 1 Cy5-tRNA^{Phe} pulse or >1 Cy5-tRNA^{Phe} pulse sampling to the long rotated state pause at codon Lys7. There is a significant number of

ribosomes exhibiting >1 Cy5-tRNA^{Phe} pulse even when there is only one Phe codon, suggesting that even without frameshifting, many of the ribosomes still pause in an uncoupled rotated state at Lys7, where tRNA^{Phe} samples the exposed UUU codon in the A site. Number of molecules analyzed n = 106.

(c) The arrival time of the first tRNA sampling to the long stalled codon for wild-type mRNA (with Cy5-tRNA^{Lys}) and AAG(UUU) with Cy5-tRNA^{Phe} are the same. Although frameshifting in principle could occur through an incomplete +2 translocation[9,10] with weakened codon-anticodon-ribosome interactions and the final reading-frame determined through the Lys8 tRNA^{Lys} sampling in the −1 frame, our data support +3 translocation that weakens codon-anticodon-ribosome interactions followed by tRNA sampling and accommodation that defines the reading frame and shifts −1 through effects of the hairpin and internal-SD interaction. For +2 translocation, we would expect to see tRNA sampling to both −1 frame and the 0 frame of A-site codon. For the AAG(UUU) mutant, tRNA^{Phe} will sample the 0 frame $U_{25}U_{26}U_{27}$, while tRNA^{Ile} will sample the −1 frame $A_{24}U_{25}U_{26}$. Since, Cy5-tRNA^{Phe} arrival times and lifetimes for sampling to the AAG(UUU) mutant match Cy5-tRNA^{Lys} arrival times and lifetimes for the wild-type sequence, there is likely no competition between tRNA^{Phe} and tRNA^{Ile} suggesting that the AUU codon is not initially exposed for tRNA^{Ile} sampling. Furthermore, for the +2 model, we would not expect a AAG(UUU) mutation to lead to a decrease in frameshifting efficiency. Thus, our results favor a +3 translocation followed by a −1 shift driven by sampling, accommodation and base-pairing stability. Unfortunately, our single-molecule assay is blind to the actual movement of the ribosome on the mRNA, so the details of this mechanism will require further exploration. See Extended Data Fig. 10 for possible implications for heterogeneous frameshift products observed previously[28]. Error bars, s.e. Number of molecules analyzed n = 212, n = 106.

(d) Mean sampling lifetime and mean sampling arrival time for Cy5-tRNA^{Phe} to the Phe8 codon for the AAG(UUU) mutant. The arrival time and lifetime are the same as Cy5-tRNA^{Lys} sampling to the Lys8 codon for the *dnaX* wild-type sequence. Number of molecules analyzed n = 106.

(e) Example trace for Cy5-tRNA^{Lys} transit through the *dnaX* frameshift mRNA AAG(UUU) mutant. For the AAG(UUU) mutant, we see only three Lys pulses, as expected, since the fourth Lys codon (Lys8) is mutated to a Phe codon. Most of the ribosomes (~80%) exhibit only three Cy5-tRNA^{Lys} pulses, indicating that the additional Cy5-tRNA^{Lys} sampling pulses we saw characteristic of frameshifting are indeed sampling to the Lys8 codon. Sampling now is by tRNA^{Phe}, which are dark and invisible to our observations. The time between pulses are consistent with both the wild-type sequence and AAG(AAA) mutant. The lifetime of the third pulse (at Lys7) is long, consistent with the long pause at that codon. Number of molecules analyzed n = 318. Error bars, s.e.

(f) Example trace for Cy5-tRNA^{Lys} transit through the *dnaX* frameshift mRNA AAG(AAC) mutant. For the AAG(AAC) mutant, we see mostly only three Lys pulses (~75%) since the fourth Lys codon (Lys8) is mutated to a Asn codon. Number of molecules analyzed n = 406. This further argues against the +2 translocation model (see part (c)). For +2 translocation, we would expect to see long Lys-tRNA sampling to the −1 frame AAA codon, which is not observed significantly. The additional Cy5-tRNA^{Lys} pulses have a shorter lifetime and longer arrival time when compared with the translation of the wild-type mRNA, suggesting

that these pulses are non-cognate sampling to the AAC codon in the 0 frame or sampling unstably to the AAA codon in the −1 frame. Even though our data supports a +3 translocation followed by a −1 slippage, multiple frameshifting pathways probably occurs. The details of this mechanism will require further exploration.

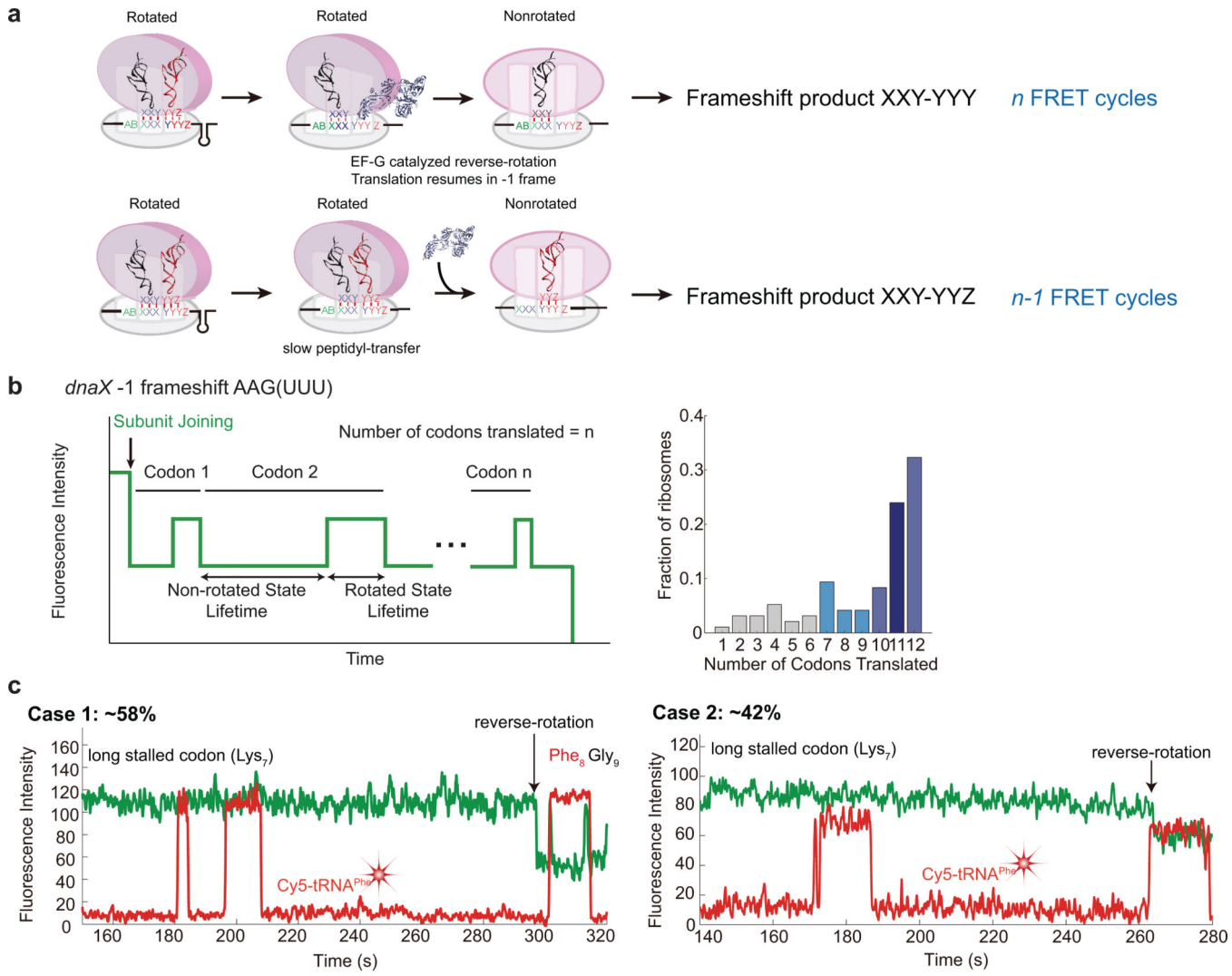

Extended Data Figure 10. Hetereogeneous frameshift products

(a) Two different protein products are possible after −1 frameshifting, dependent on whether peptide bond formation occurs during sampling in the −1 or 0 frame. For the first scenario, tRNA sampling to the last three nucleotides of the slippery sequence (YYZ) redefines the ribosome in the −1 frame (YYY), after which the tRNA dissociates to leave an empty A-site codon. After the long rotated state is reverse-rotated by EF-G, $tRNA^{YYY}$ decodes that codon normally, creating a frameshift product denoted by XXY-YYY. For the second scenario, peptide bond formation occurs after slippage of $tRNA^{YYZ}$ into the −1 frame; peptide-bond formation occurs slowly, since the P- and A-site tRNAs would likely not be positioned correctly in the rotated ribosomal conformation. EF-G would then normally and rapidly

resolve the newly-created A/P hybrid state and the ribosome reverse-rotates. In this case, the frameshift product will be denoted by XXY-YYZ.

(b) Histogram of the fraction of ribosomes translating to a particular codon for the *dnaX* −1 frameshift AAG(UUU) mRNA, with a schematic. Since the frameshifting percentage for the AAG(UUU) sequence is low, we see that most of the ribosomes translate up to 12 codons where the 0 frame stop codon is. Though, there is a significant number of ribosomes that translate to 11 codons (~25%), compared to ~5% for our previous experiments. There are two possible scenarios for $tRNA^{Phe}$ sampling to the long rotated-state pause to codon Phe8. In the first case, the $tRNA^{Phe}$ defines the reading frame and falls off, after which the ribosome resolves itself through the action of EF-G, followed by the normal decoding of Phe codon at codon 8. In this case, we get 12 cycles of low-high-low FRET intensity, and hence 12 codons translated by our signal. In the second case, the $tRNA^{Phe}$ defines the reading frame, followed by slow peptide bond formation. After peptide bond formation, the ribosome returns to the canonical hybrid and rotated state, for which EF-G then catalyzes reverse rotation. In this case, one low-high-low FRET cycle is missed, so we count 11 codons translated by our signal. This explains the heterogeneity in frameshift products observed in many frameshift systems[28]. Number of molecules analyzed $n = 353$.

(c) Example traces of Cy5-$tRNA^{Phe}$ (red) sampling to the long rotated-state pause at codon Lys7 correlated with Cy3B/BHQ conformational FRET signal (green), showing the two possible scenarios for tRNA sampling. Case 1 (as described in part (a)) leads to correlation of tRNA arrival and ribosome rotation after the long rotated state pause whereas case 2 leads to overlap of a $tRNA^{Phe}$ pulse with the reverse-rotation of the long pause. Both scenarios occur when translating the AAG(UUU) mutant, with ~58% of ribosomes for case 1 and 42% for case 2. For the 2nd case, the time between the last Cy5-$tRNA^{Phe}$ arrival and the ribosome reverse-rotation is 27.2 s, much longer than the 7.7 s during normal decoding and translocation, suggesting a slow peptidyltransfer reaction. Our results provide a possible explanation for why heterogeneous frameshifting products are observed in many frameshifting systems. Number of molecules analyzed $n = 55$.

ACKNOWLEDGEMENTS

This work was supported by US National Institutes of Health (NIH) grant GM51266 to J.C., A.T., and J.D.P., by NIH grant GM099687 to A.P., S.E.O'L, and J.D.P., Wenner-Gren Foundation to M.J, and by a Stanford Interdisciplinary Graduate Fellowship to J.C. The authors thank David Hsu and Ravindra Dalal (Pacific Biosciences Inc.) for their assistance on the ZMW instrumentation. J.C. would like to thank I Lin for support.

References

1. Jenner LB, Demeshkina N, Yusupova G, Yusupov M. Structural aspects of messenger RNA reading frame maintenance by the ribosome. Nature structural & molecular biology. 2010; 17:555–560.
2. Tinoco I Jr, Kim HK, Yan S. Frameshifting dynamics. Biopolymers. 2013; 99:1147–1166. [PubMed: 23722586]
3. Tsuchihashi Z, Kornberg A. Translational frameshifting generates the gamma subunit of DNA polymerase III holoenzyme. Proceedings of the National Academy of Sciences of the United States of America. 1990; 87:2516–2520. [PubMed: 2181440]
4. Plant EP, et al. The 9-A solution: how mRNA pseudoknots promote efficient programmed −1 ribosomal frameshifting. RNA. 2003; 9:168–174. [PubMed: 12554858]
5. Baranov PV, Gesteland RF, Atkins JF. P-site tRNA is a crucial initiator of ribosomal frameshifting. RNA. 2004; 10:221–230. [PubMed: 14730021]

6. Horsfield JA, Wilson DN, Mannering SA, Adamski FM, Tate WP. Prokaryotic ribosomes recode the HIV-1 gag-pol-1 frameshift sequence by an E/P site post-translocation simultaneous slippage mechanism. Nucleic acids research. 1995; 23:1487–1494. [PubMed: 7784201]
7. Lopinski JD, Dinman JD, Bruenn JA. Kinetics of ribosomal pausing during programmed −1 translational frameshifting. Molecular and cellular biology. 2000; 20:1095–1103. [PubMed: 10648594]
8. Jacks T, Madhani HD, Masiarz FR, Varmus HE. Signals for ribosomal frameshifting in the Rous sarcoma virus gag-pol region. Cell. 1988; 55:447–458. [PubMed: 2846182]
9. Namy O, Moran SJ, Stuart DI, Gilbert RJ, Brierley I. A mechanical explanation of RNA pseudoknot function in programmed ribosomal frameshifting. Nature. 2006; 441:244–247. [PubMed: 16688178]
10. Weiss RB, Dunn DM, Shuh M, Atkins JF, Gesteland RFE. coli ribosomes re-phase on retroviral frameshift signals at rates ranging from 2 to 50 percent. The New biologist. 1989; 1:159–169. [PubMed: 2562219]
11. Leger M, Dulude D, Steinberg SV, Brakier-Gingras L. The three transfer RNAs occupying the A, P and E sites on the ribosome are involved in viral programmed −1 ribosomal frameshift. Nucleic acids research. 2007; 35:5581–5592. [PubMed: 17704133]
12. Larsen B, Gesteland RF, Atkins JF. Structural probing and mutagenic analysis of the stem-loop required for Escherichia coli dnaX ribosomal frameshifting: programmed efficiency of 50%. Journal of molecular biology. 1997; 271:47–60. [PubMed: 9300054]
13. Larsen B, Wills NM, Gesteland RF, Atkins JF. rRNA-mRNA base pairing stimulates a programmed −1 ribosomal frameshift. Journal of bacteriology. 1994; 176:6842–6851. [PubMed: 7961443]
14. Chen J, et al. High-throughput platform for real-time monitoring of biological processes by multicolor single-molecule fluorescence. Proceedings of the National Academy of Sciences of the United States of America. 2013 doi:10.1073/pnas.1315735111.
15. Kim HK, et al. A frameshifting stimulatory stem loop destabilizes the hybrid state and impedes ribosomal translocation. Proceedings of the National Academy of Sciences of the United States of America. 2014; 111:5538–5543. [PubMed: 24706807]
16. Chen J, Petrov A, Tsai A, O'Leary SE, Puglisi JD. Coordinated conformational and compositional dynamics drive ribosome translocation. Nature structural & molecular biology. 2013; 20:718–727.
17. Chen J, Tsai A, Petrov A, Puglisi JD. Nonfluorescent quenchers to correlate single-molecule conformational and compositional dynamics. Journal of the American Chemical Society. 2012; 134:5734–5737. [PubMed: 22428667]
18. Aitken CE, Puglisi JD. Following the intersubunit conformation of the ribosome during translation in real time. Nature structural & molecular biology. 2010; 17:793–800.
19. Tsuchihashi Z, Brown PO. Sequence requirements for efficient translational frameshifting in the Escherichia coli dnaX gene and the role of an unstable interaction between tRNA(Lys) and an AAG lysine codon. Genes & development. 1992; 6:511–519. [PubMed: 1547945]
20. Bertrand C, Prere MF, Gesteland RF, Atkins JF, Fayet O. Influence of the stacking potential of the base 3' of tandem shift codons on −1 ribosomal frameshifting used for gene expression. RNA. 2002; 8:16–28. [PubMed: 11871658]
21. Johansson M, Zhang J, Ehrenberg M. Genetic code translation displays a linear trade-off between efficiency and accuracy of tRNA selection. Proceedings of the National Academy of Sciences of the United States of America. 2012; 109:131–136. [PubMed: 22190491]
22. Tourigny DS, Fernandez IS, Kelley AC, Ramakrishnan V. Elongation factor G bound to the ribosome in an intermediate state of translocation. Science. 2013; 340:1235490. [PubMed: 23812720]
23. Hughes D, Atkins JF, Thompson S. Mutants of elongation factor Tu promote ribosomal frameshifting and nonsense readthrough. The EMBO journal. 1987; 6:4235–4239. [PubMed: 3327691]
24. Qu X, et al. The ribosome uses two active mechanisms to unwind messenger RNA during translation. Nature. 2011; 475:118–121. [PubMed: 21734708]
25. Liu CY, Qureshi MT, Lee TH. Interaction strengths between the ribosome and tRNA at various steps of translocation. Biophysical journal. 2011; 100:2201–2208. [PubMed: 21539788]

26. Valle M, et al. Locking and unlocking of ribosomal motions. Cell. 2003; 114:123–134. [PubMed: 12859903]
27. Qin P, Yu D, Zuo X, Cornish PV. Structured mRNA induces the ribosome into a hyper-rotated state. EMBO reports. 2014; 15:185–190. [PubMed: 24401932]
28. Jacks T, et al. Characterization of ribosomal frameshifting in HIV-1 gag-pol expression. Nature. 1988; 331:280–283. [PubMed: 2447506]
29. Liao PY, Choi YS, Dinman JD, Lee KH. The many paths to frameshifting: kinetic modelling and analysis of the effects of different elongation steps on programmed −1 ribosomal frameshifting. Nucleic acids research. 2011; 39:300–312. [PubMed: 20823091]
30. Uemura S, et al. Real-time tRNA transit on single translating ribosomes at codon resolution. Nature. 2010; 464:1012–1017. [PubMed: 20393556]
31. Frank J, Agrawal RK. A ratchet-like inter-subunit reorganization of the ribosome during translocation. Nature. 2000; 406:318–322. [PubMed: 10917535]
32. Agirrezabala X, et al. Visualization of the hybrid state of tRNA binding promoted by spontaneous ratcheting of the ribosome. Molecular cell. 2008; 32:190–197. [PubMed: 18951087]
33. Munro JB, Altman RB, O'Connor N, Blanchard SC. Identification of two distinct hybrid state intermediates on the ribosome. Molecular cell. 2007; 25:505–517. [PubMed: 17317624]
34. Blanchard SC, Gonzalez RL, Kim HD, Chu S, Puglisi JD. tRNA selection and kinetic proofreading in translation. Nature structural & molecular biology. 2004; 11:1008–1014.
35. Moazed D, Noller HF. Intermediate states in the movement of transfer RNA in the ribosome. Nature. 1989; 342:142–148. [PubMed: 2682263]
36. Cornish PV, Ermolenko DN, Noller HF, Ha T. Spontaneous intersubunit rotation in single ribosomes. Molecular cell. 2008; 30:578–588. [PubMed: 18538656]
37. Marshall RA, Dorywalska M, Puglisi JD. Irreversible chemical steps control intersubunit dynamics during translation. Proceedings of the National Academy of Sciences of the United States of America. 2008; 105:15364–15369. [PubMed: 18824686]
38. Dorywalska M, et al. Site-specific labeling of the ribosome for single-molecule spectroscopy. Nucleic acids research. 2005; 33:182–189. [PubMed: 15647501]
39. Marshall RA, Aitken CE, Puglisi JD. GTP hydrolysis by IF2 guides progression of the ribosome into elongation. Molecular cell. 2009; 35:37–47. [PubMed: 19595714]
40. Blanchard SC, Kim HD, Gonzalez RL Jr, Puglisi JD, Chu S. tRNA dynamics on the ribosome during translation. Proceedings of the National Academy of Sciences of the United States of America. 2004; 101:12893–12898. [PubMed: 15317937]
41. Wen JD, et al. Following translation by single ribosomes one codon at a time. Nature. 2008; 452:598–603. [PubMed: 18327250]
42. Li GW, Oh E, Weissman JS. The anti-Shine-Dalgarno sequence drives translational pausing and codon choice in bacteria. Nature. 2012; 484:538–541. [PubMed: 22456704]
43. Aitken CE, Marshall RA, Puglisi JD. An oxygen scavenging system for improvement of dye stability in single-molecule fluorescence experiments. Biophysical journal. 2008; 94:1826–1835. [PubMed: 17921203]

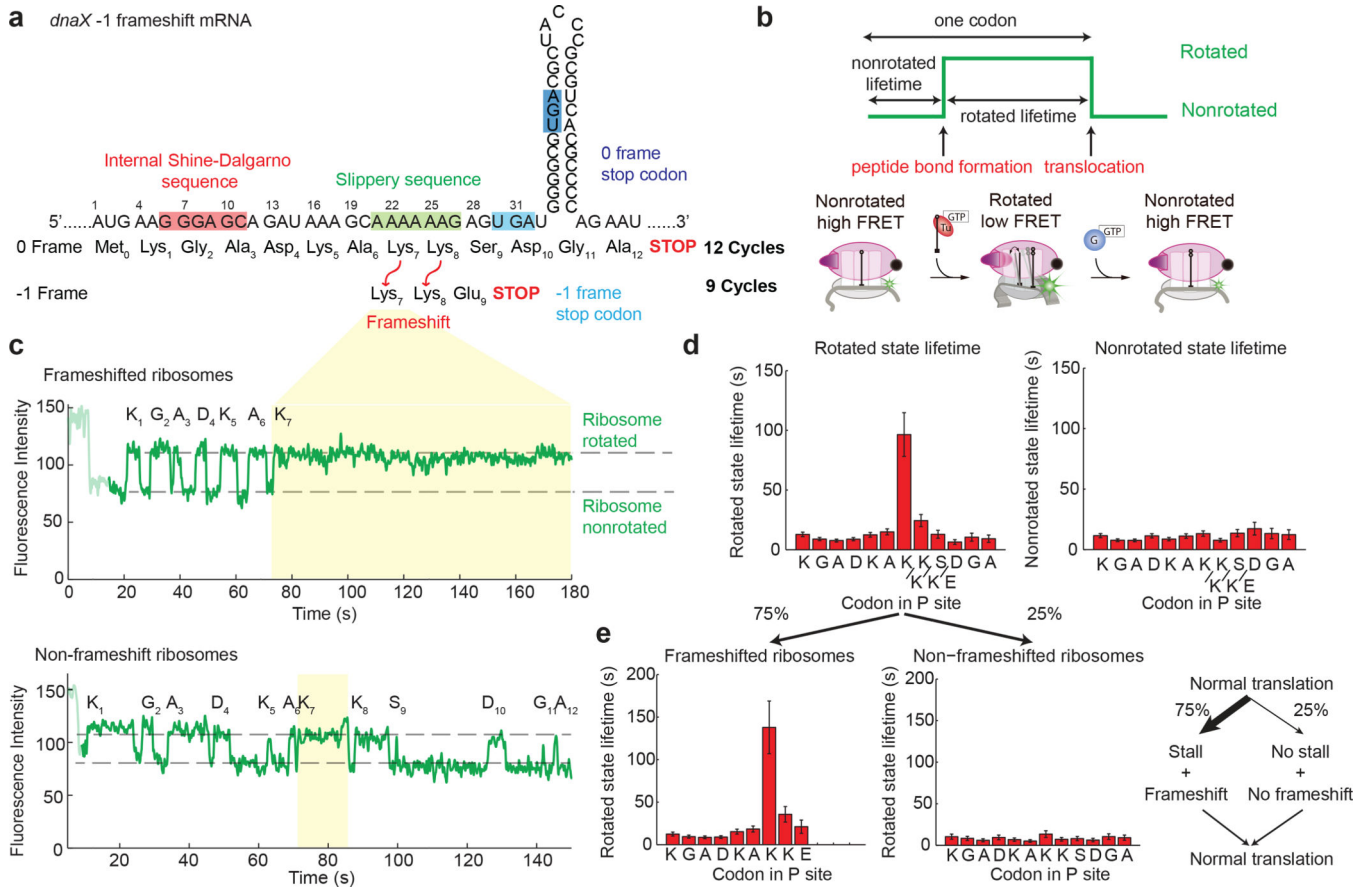

Figure 1. Frameshifting is characterized by a long rotated-state pause

(a) Schematic of the mRNA used in this study, modified from the *dnaX* gene.

(b) Schematic of the Cy3B/BHQ conformational FRET signal, with each low-high-low Cy3B intensity cycle representing a ribosome elongating one codon.

(c) Example traces of Cy3B (green) fluorescent intensity for frameshifted and non-frameshifted ribosomes translating with 80 nM EF-G and 1 μM $tRNA_{tot}$ TC. Codon Lys7 of the frameshift site is shaded yellow.

(d) The mean rotated-state lifetime and nonrotated state lifetime. The nonrotated state lifetime is constant. There is a 10-fold increase in rotated state lifetime at codon Lys7. *n* = 256. Error bars, s.e.

(e) By parsing the rotated state lifetimes in (c) into ribosomes that frameshift (75%) and ribosomes that do not frameshift (25%), we see only the rotated state pause at codon Lys7 for frameshifted ribosomes.

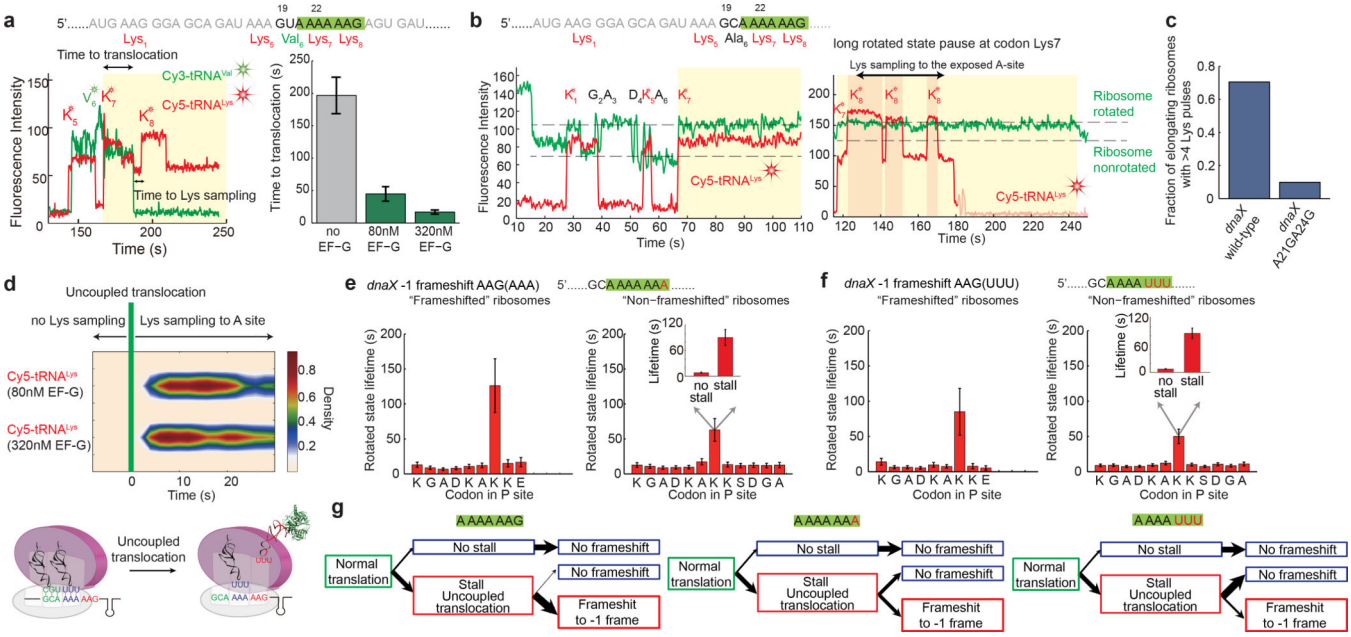

Figure 2. tRNA samples the rotated state after uncoupled translocation and defines the reading frame

(a) Sample trace and time to translocation at the frameshift site, which is estimated by Cy3-tRNA^{Val} (green) departure from the E-site during frameshifting relative to the arrival of Cy5-tRNA^{Lys} (red) at codon Lys7 (shaded in yellow) on a GCA$_{21}$ (Ala) to GUA$_{21}$ (Val) mRNA mutant. From left to right, n = 337, 449, 455. Error bars, s.e.

(b) Example trace of correlation of the Cy3B/BHQ ribosome conformational signal (green) with Cy5-tRNA^{Lys} (red), confirming the long pause at codon Lys7 (shaded yellow). Upon reaching codon Lys7, additional tRNA^{Lys} pulses sample codon Lys8 in the A site (shaded red), which results in a buildup of Cy5 intensity from the two Cy5-tRNA^{Lys} in the A and P sites of the ribosome.

(c) Fraction of elongating ribosomes exhibiting >4 Lys pulses (additional sampling pulses) for the frameshift wild-type mRNA and the A21GA24G mutant. From left to right, n = 179 and n = 147.

(d) Two-dimensional density plot of Cy5-tRNA^{Lys} sampling to codon Lys8 in the A site post-synchronized to the time of translocation (indicated by the green line). The sampling of tRNA^{Lys} at Lys8 only begins after translocation.

(e) Rotated and nonrotated state lifetimes for the slippery sequence mutant ($A_{25}A_{26}G_{27}$ codon to AAA). There is now an extra subpopulation of ribosomes with a long rotated-state pause but does not lead to frameshifting. n = 310. Error bars, s.e.

(f) Mutation of the last $A_{25}A_{26}G_{27}$ codon to UUU (Phe). Similar to (e), there are two subpopulations within the non-frameshifted ribosomes. n = 353. Error bars, s.e.

(g) Pathways of frameshifting for the various slippery sequence mutants, indicating how tRNA sampling defines the final reading frame.

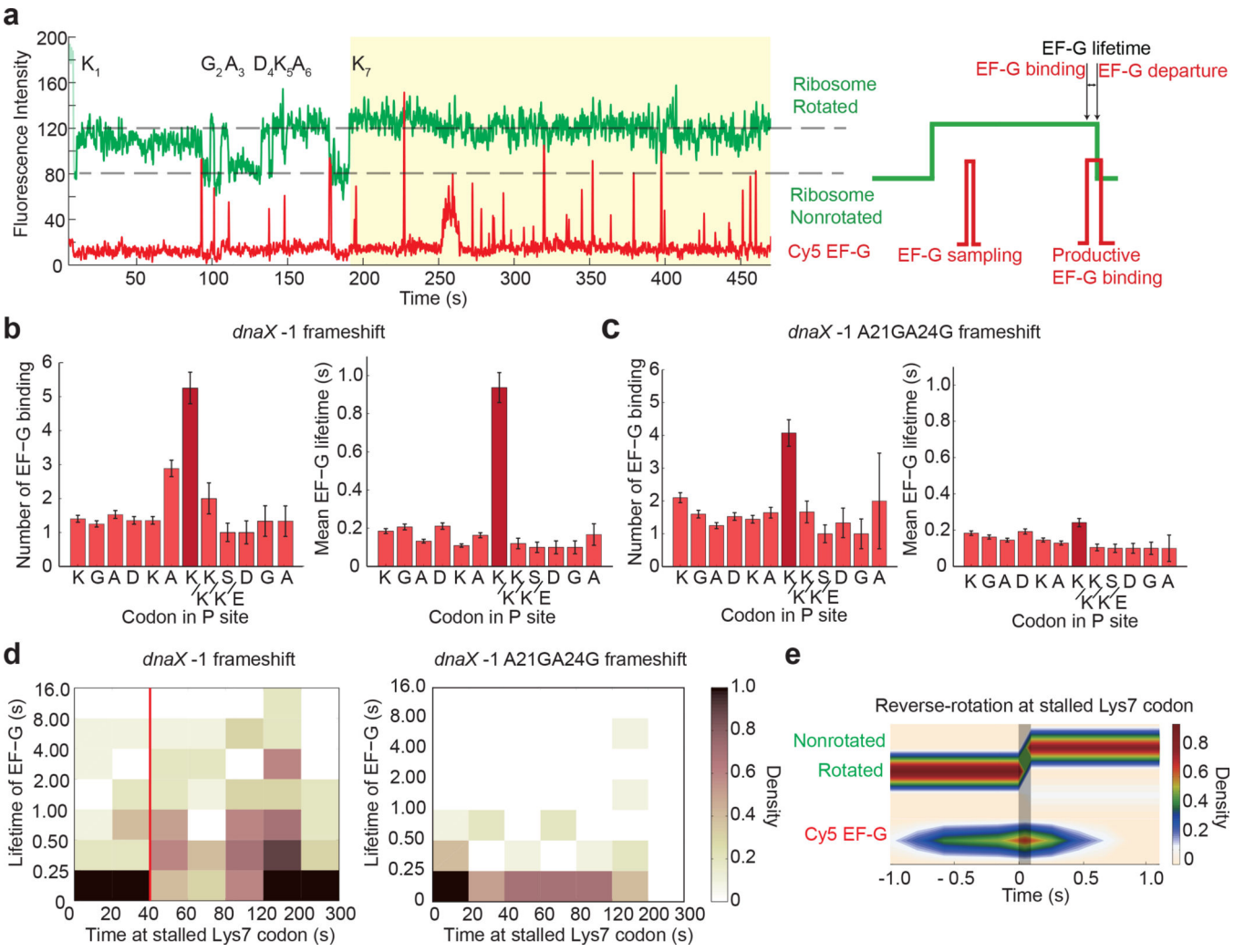

Figure 3. EF-G samples and resolves the uncoupled rotated state after frameshifting

(a) Sample trace and schematic of the correlation of Cy3B/BHQ ribosome conformational signal (green) with Cy5-EF-G binding (red). Cy5-EF-G pulses are correlated with ribosome reverse-rotation at each codon. At the rotated state pause at codon Lys7 (shaded in yellow), multiple EF-G sampling events with long dwell times can be observed.

(b) EF-G sampling and EF-G lifetimes for each codon for the wild-type frameshift mRNA. There is an increased number of sampling as well as increased mean EF-G lifetime at codon Lys7. *n* = 122. Error bars, s.e.

(c) For the A21GA24G mutant mRNA, there is a slight increase in number of sampling at Lys7 codon due to the increase in energy barrier from the hairpin and internal-SD interaction, but the long EF-G lifetime disappears. *n* = 157. Error bars, s.e.

(d) Two-dimensional histogram plotting time at the stalled rotated state at codon Lys7 vs. lifetime of EF-G. Longer EF-G lifetimes only appear after uncoupled translocation, as roughly indicated by the red line. For the A21GA24G mutant, no long EF-G lifetimes are observed. *n* = 122, *n* = 157.

(e) Postsynchronization plot correlating ribosome reverse-rotation at the Lys7 codon with EF-G. *n* = 436.

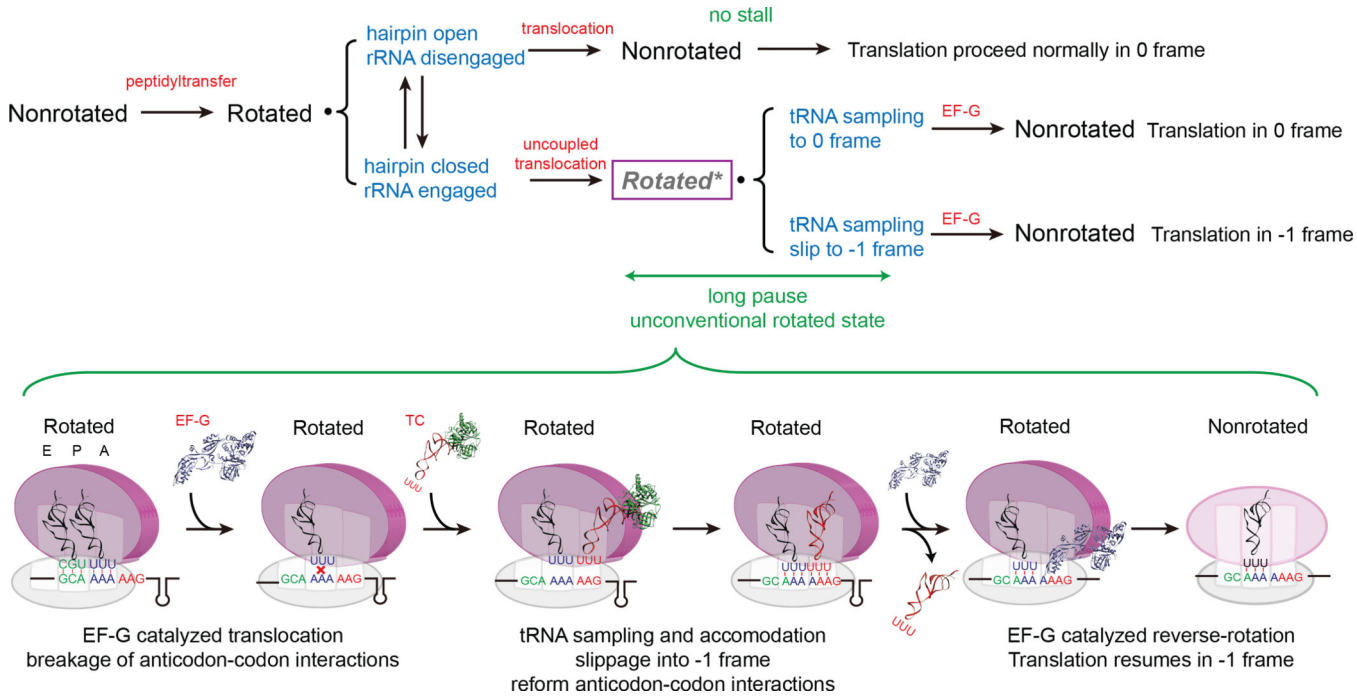

Figure 4. Branchpoint of pathways and mechanism of *dnaX* −1 frameshifting

The first branchpoint during frameshifting is likely due to the stochastic interaction of the ribosome with the hairpin in an open or closed state, and/or formation of the SD-antiSD pairing, that represent the shunt to either pausing or normal translation. Translocation of the paused ribosomes under the slippery sequence with the tension caused by the hairpin and SD leads to +3 translocation, but uncoupled from reverse ribosomal rotation, creating a non-canonical intermediate in translation (denoted ***Rotated****). The uncoupled translocation exposes the A site, to which $tRNA^{Lys}$ and EF-G sample. $tRNA^{Lys}$ sampling and accommodation to the AAG codon stimulates the ribosome to slip into the −1 frame. Finally, EF-G catalyzes the final reverse-rotation, after which the ribosome resumes normal translation.